

## SNS donors as mimic to enzymes, chemosensors, and imaging agents

Poonam Kaswan<sup>a</sup>, Preeti Oswal<sup>b</sup>, Arun Kumar<sup>b</sup>, Chandra Mohan Srivastava<sup>a</sup>, Dipti Vaya<sup>a</sup>,  
Varun Rawat<sup>c</sup>, Kamal Nayan Sharma<sup>a</sup>, Gyandshwar Kumar Rao<sup>a,\*</sup>

<sup>a</sup> Department of Chemistry, Biochemistry and Forensic Science, Amity School of Applied Sciences, Amity University Haryana, 122413, India

<sup>b</sup> Department of Chemistry, School of Physical Sciences, Doon University, Dehradun, 248012, India

<sup>c</sup> Faculty of Exact Sciences, School of Chemistry, Tel Aviv University, 69978, Israel

### ARTICLE INFO

#### Keywords:

SNS complex  
Bioimaging/biolabelling  
Model complexes  
Chemosensor  
Enzyme mimicking

### ABSTRACT

This review summarizes multidentate SNS ligands as enzyme imitating models, chemosensors, and bioimaging agents. Due to the obvious prevalence of bioactive sulfur and nitrogen donors, SNS ligands have a substantial biological value. Sulfur-based tridentate ligands are frequently used to mimic the active sites of metalloproteins to truly comprehend enzyme active sites and have been used as building blocks to construct innovative model complexes. Metal complexes of such ligands, including Cu, Ni, Zn, Fe, Mo, and Co have been thoroughly investigated to imitate the enzymes. Chemosensors based on SNS donor and their functionalized polymers used for cation/anion and molecule detection, such as Al<sup>3+</sup>, Pb<sup>2+</sup>, Hg<sup>2+</sup>, F<sup>-</sup>, and glucose, have also been reviewed. The carcinogenic and psychiatric activity of trace metal <sup>99m</sup>Tc and <sup>186</sup>Re complexes with tridentate SNS moiety has been discussed *in vivo*, *in vitro*, and *in silico* for brain ailments, schizophrenic, and other neurodegenerative problems. Ligands having SNS moiety used as a radiotracer in bioimaging have been discussed. Other biological activity observed in gold complexes of SNS ligands, which have been administered as an antiparasitic medicine to manage Chagas disease, malaria, and other infectious diseases, has also been covered.

### 1. Introduction

A SNS tridentate ligand system consists of biologically active elements such as 'S' and 'N'. Complexes of SNS donor ligands have been widely studied as catalysts, sensors, and bio-labeling agents; however, they have been less explored for their biological applications. The complexes of SNS ligands have attracted considerable attention due to their multifunctional, flexible, and stereoelectronic environment [1-3]. Such complexes have already been used in the manufacturing of industrial, pharmacological and horticultural chemicals [4-10], solar fuel [11], resins [12], and CO<sub>2</sub> fixation [6,13]. Protein and enzyme shared similar nitrogen and sulfur donors, and thus such complexes have a wide spectrum of biological consequences and have been leveraged to imitate enzymes [13-15]. Model complexes are artificial enzymes that represent enzymes and depict enzyme activity [16,17], giving structural and spectroscopic insights on metalloenzyme active sites [18,19], oxidation state etc. (see Fig. 1) Different sulfur and nitrogen-containing model complexes have been designed with Cu [20-22], Ni [23-26], Fe [27-29], Zn [30,31], and Co [32] metal ions, forming an active site that is important in the structure and activity of natural enzymes [33,34].

Based on the structure and reactivity of such complexes, the activity of a similar enzyme can be mimicked. Various complexes containing thiosemicarbazone [22,35], thiol [36,37], thiophenol [38-40] or thiocarbamide [41] moiety have found to show similar activity as compared to natural systems such as Hydrogenases [29,42], LADH [43], Cytochrome C, Oxidase [44], LarA [34,45], Nitrogenase [39] and Oxygenase [46-48] (see Fig. 2).

Multidentate ligands with different metals have characteristic properties of luminescence which depend on the nature of metal as well as a ligand [49-51]. These complexes have been employed as chemosensors or biosensors. Their luminescence behavior is attributed due to either metal to ligand charge transfer (MLCT) or ligand to metal charge transfer (LMCT), or metal to metal to ligand charge transfer [52-54]. Transition metal complexes of spiropyran, spiroxazine, azobenzene, and diarylethenes ligands have been found to show significant photoelectric effect and good sensing properties [55]. This is due to their suitable bandgap, atomically flat surface topography, and the absence of dangling bonds and strong covalent bonds within the layers [56]. Several chemosensors containing sulfur and nitrogen donor atoms have been developed for metal ion detection [57-60]. Tridentate SNS ligands have been utilized for the detection and removal of toxic metal due to

\* Corresponding author.

E-mail address: [gk rao@ggn.amity.edu](mailto:gk rao@ggn.amity.edu) (G. Kumar Rao).

## Nomenclature

### Abbreviations

LADH	Liver alcohol dehydrogenase
BNAH	4-Dihydronicotinamide
DMPE	1,2-Bisdimethylphosphinoethane
PET	Photoemission tomography
<sup>99m</sup> Tc	The nuclear isomer of technetium
<sup>186/188</sup> Re	The nuclear isomer of rhenium
SAR	Structure-activity relation
IC <sub>50</sub>	Half maximal inhibitory concentration
ST/CB	Stratum/cerebellum ratio
DAMP	Dimethylaminomethyl phenyl
CNxylyl	2,6-Dimethylphenyl isocyanide
Dmpm	Bis(dimethylphosphino)methane
Tbtmp	2,6-bis( <i>tert</i> -butylthiomethyl)pyridine
BTP	5-Amino- <i>N</i> , <i>N</i> ′-bis(2,5-di(thiophen-2-yl)-1 <i>H</i> -pyrrol-1-yl)isophthalamide
HMPAO	Hexamethyl propylene amine oxime
ECD	Ethyl cysteinyl dimer
DO3A	2,2′,2″-[10-(1-[2-(2,5-di-2-thienyl-1 <i>H</i> -pyrrol-1-yl)ethyl]-1 <i>H</i> -1,2,3-triazol-4-yl)-methyl-1,4,7,10-tetraazacyclododecane-1,4,7-triyl]triacetate

their chelation ability. Such ligands can easily interact with heavy metals due to the presence of a soft “S” atom. The fluorescent sensors based on SNS moiety show turn-ON/OFF behavior [61-64] and are utilized for cation/anion and other molecule sensing and target detection (see Fig. 3).

The functional conjugated polymer of SNS moiety has drawn significant attention as chemosensors / optical devices / switches due to their high contrast ratio and fast switching capability with good selectivity and sensitivity [65-68]. Ferraris [69,70], Toppare [71,72], Yavuz [73,74] and Cihaner et al. [75-80] have reported the synthesis and polymerization of a variety of *N*-substituted SNS derivatives. These systems have been investigated for optical properties and electrochromism in phthalonitrile, phthalocyanine and luminol [73,74,80-84]. Transition metals have significant biological activity and are important in therapeutic along with diagnostics. Tc- and Re-SNS systems are excellent cell imaging agents for spotting brain and tumor cells. Tc is biological and medical friendly and is the most favorable metal for radiopharmacy due to its suitable half-life and easy availability [85-88]. Re compounds have also similar radioactive tracer capabilities and are  $\gamma$ -emitters [89]. Tc and Re complexes comprising of S and N donor atoms function as dopamine and serotonin transporter and diagnostic agents [90]. Mastrotamatis [91], Papadopoulou [92,93], Pelecanou [86,94,95], Tsoukalas [96], Pirmettis [97], and Patsis et al. [98] reported the SNS complexes as bioimaging agents. These complexes are classified into two categories namely 3 + 1 (SNS/S, SNS/N) and 3 + 2 (SNS/PO) [99-104] systems (Fig. 4).

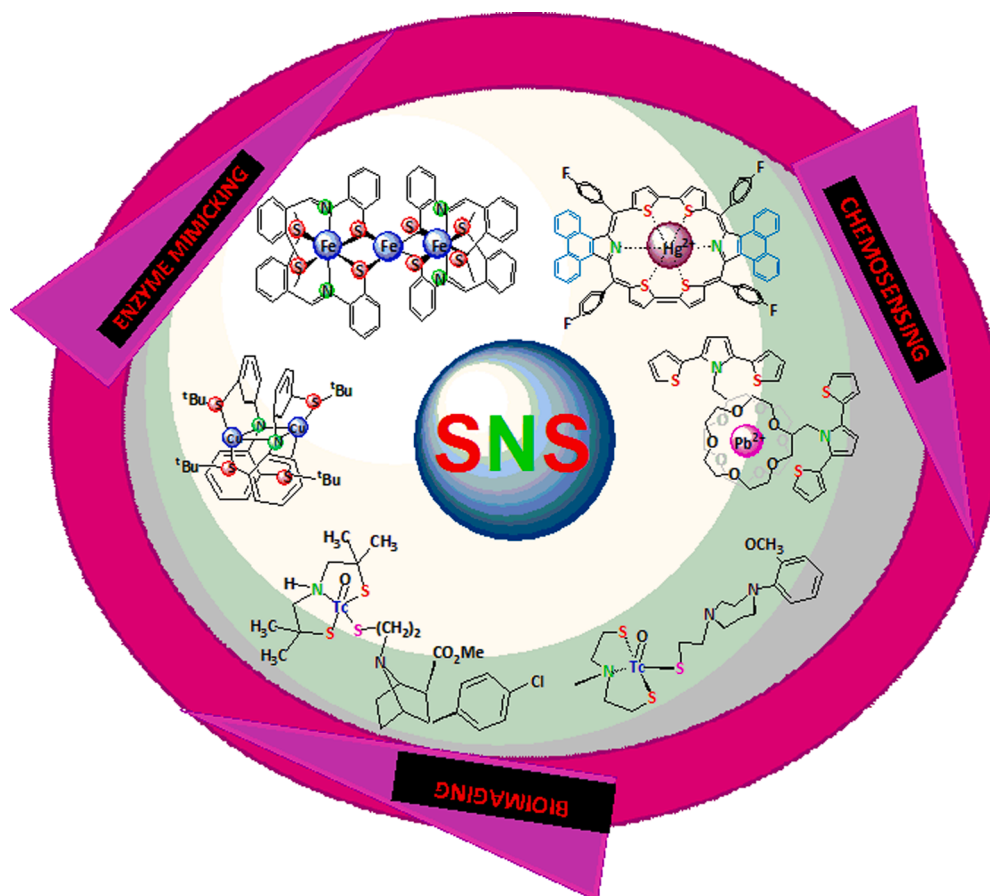


Fig. 1. Utilization of SNS complexes.

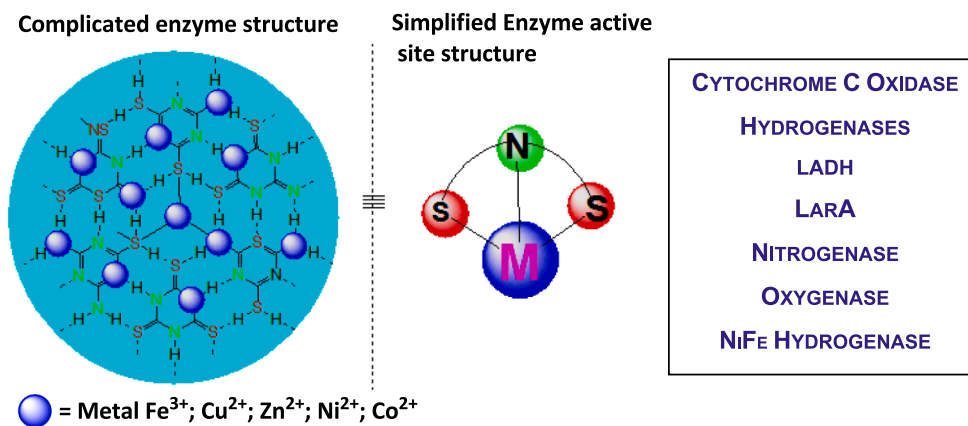


Fig. 2. Representation of complex enzyme structure and simplified SNS model complex.

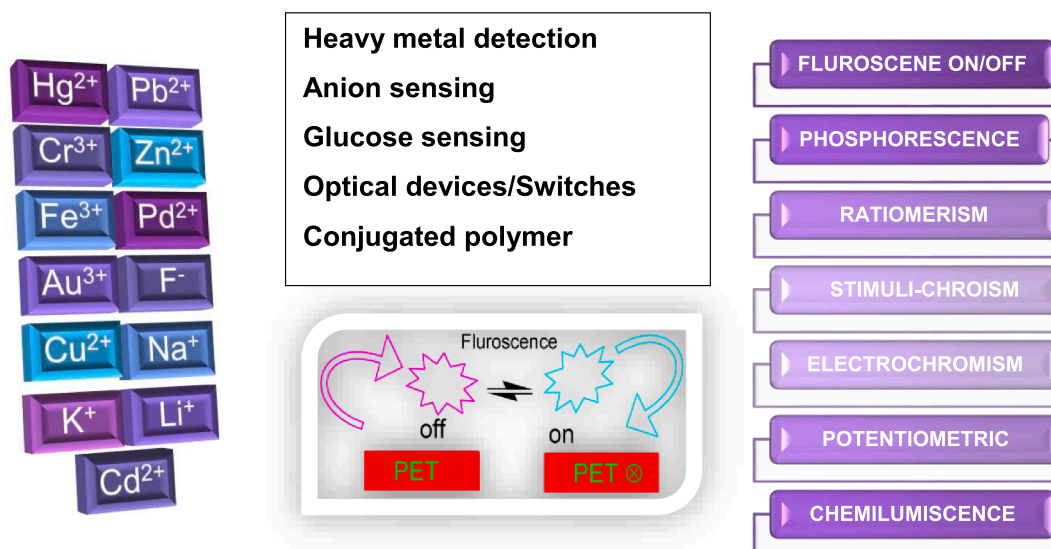


Fig. 3. SNS ligands for sensing and methods of detection.

The Re-SNS-complexes have been found to show good anticancer activity. SNS-Au complexes [105] have shown both cytotoxic and anti-protozoal effects and can target both cancers and parasitic cells. SNS system itself has the property of kinase inhibition [106-115] and is used as medicine to treat the tumor.

## 2. Model complexes-Artificial enzymes

Compounds having ligand-based redox activity, meridional binding and softer donor atoms are important to mimic metalloenzymes. Tridentate (SNS) ligand provides a unique platform for studying the reactivity of diverse Hydrogenase, Reductase, and Oxygen-atom transfer enzymes.

### 2.1. Bisthione complexes of zinc and cobalt

Liver alcohol dehydrogenase (LADH), is a zinc metalloenzyme, has a Zn(II) as a metal center. This Zn(II) metal center is pseudo-tetrahedrally ligated with a labile water molecule, one N-histidine and two S-cysteine side chains resulting in an SNS ligand environment. LADH catalyzes the oxidation of alcohols to aldehydes and ketones and reduction of ketone or an aldehyde to alcohol. To understand the catalytic activity of Zn metalloenzyme, Miecznikowski et al. [43,116-119] have synthesized the Zn-bisthione as a model complexes 1-6 (Chart 1), by using a tridentate pincer ligand based on bis-imidazole or bis-triazole.

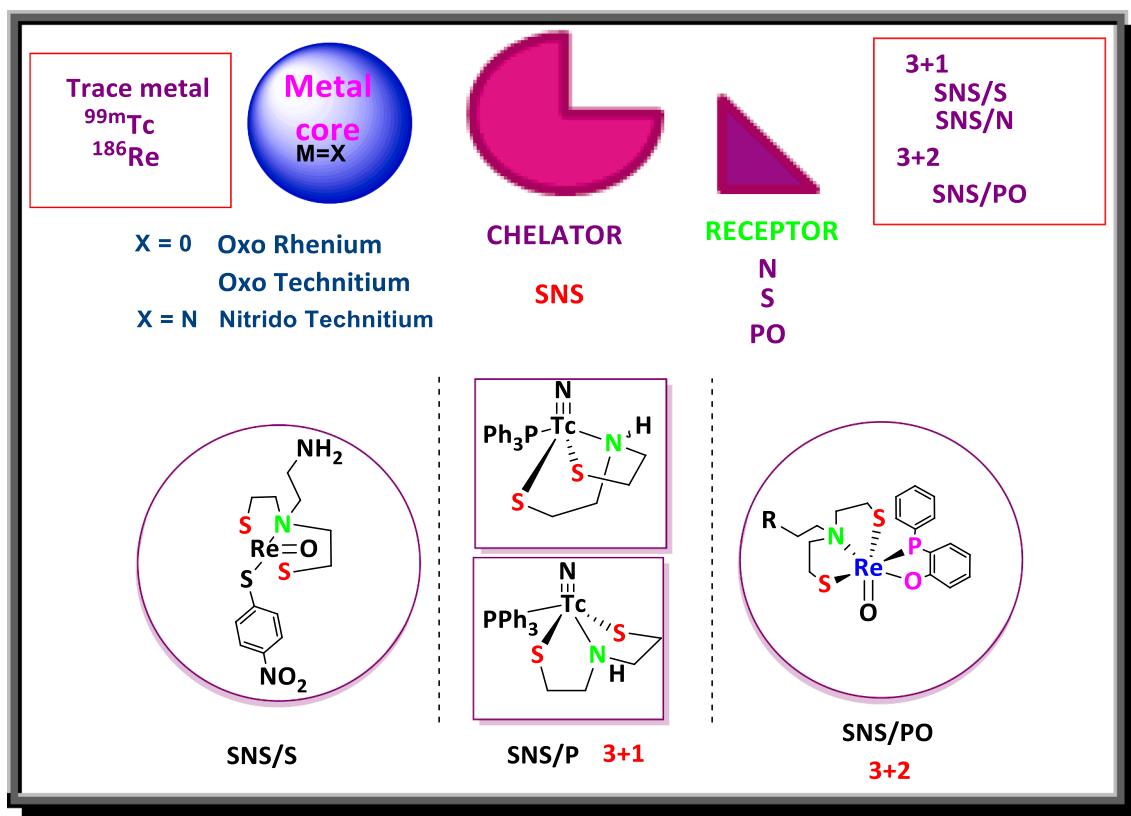
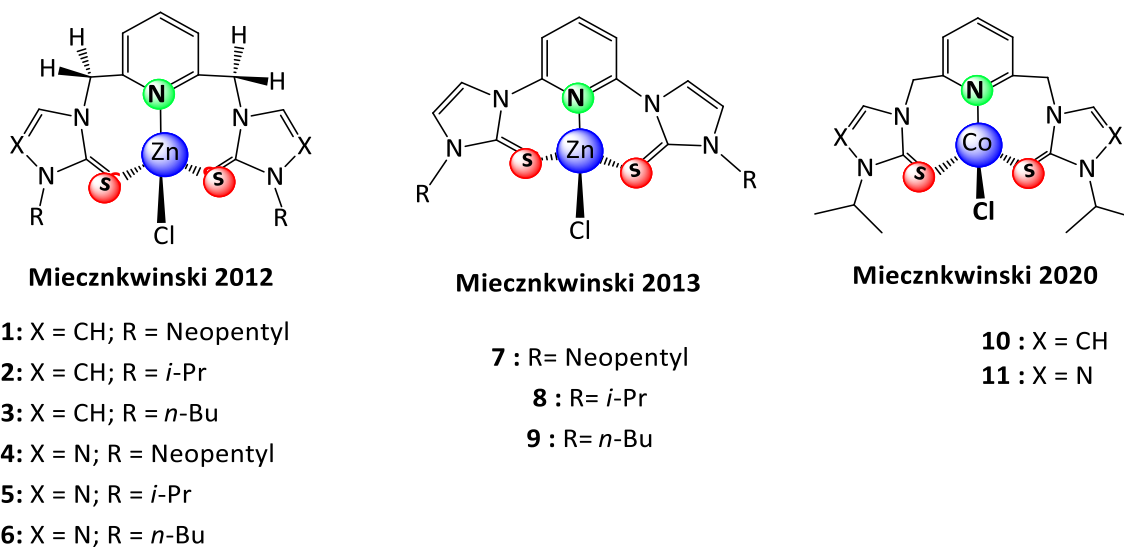
Fig. 4.  $^{99m}\text{Tc}$  - /  $^{186/188}\text{Re}$ -SNS complexes as imaging agents.

Chart 1. Zn(II)- and Co(II)-bithione complexes to mimic the activity of LADH.

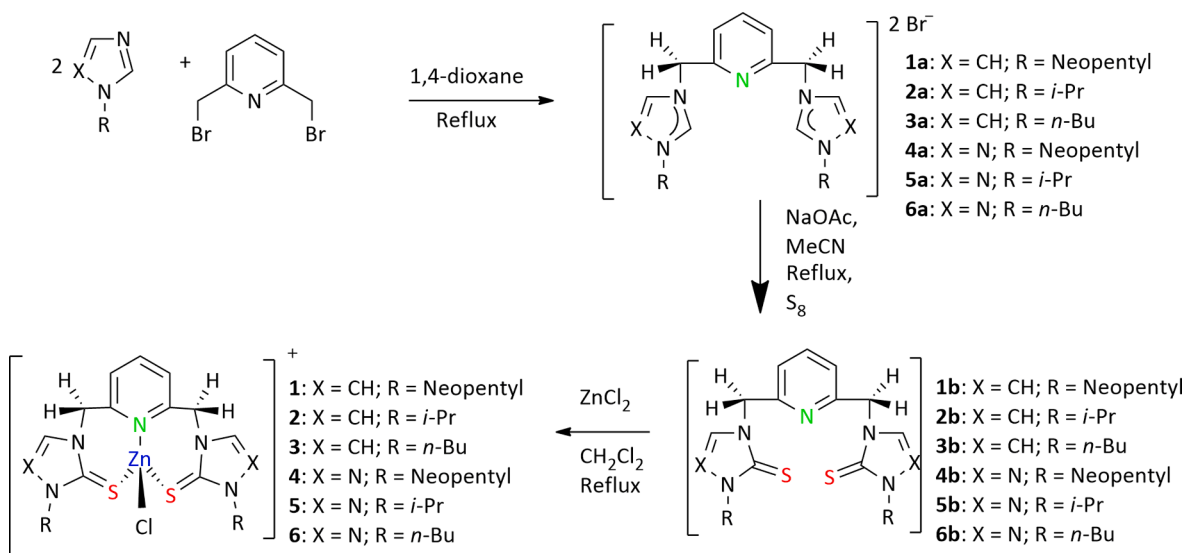
The strategy employed for the synthesis of Zn complexes (1–6) is presented in Scheme 1. These complexes served as models for the zinc active site in liver alcohol dehydrogenase. They adopted a pseudo-tetrahedral geometry and have an SNS coordination environment about the Zn center like present in LADH [117].

These Zn complexes (1–6) have been studied for the reduction of electron-poor aldehydes in presence of BNAH (Scheme 2). Furthermore, the Zn complexes of bithione based tridentate SNS pincer (7–9) have also served as model complexes. The bond lengths, bond angles, and geometry of these complexes (7–9) correlate well with those present in

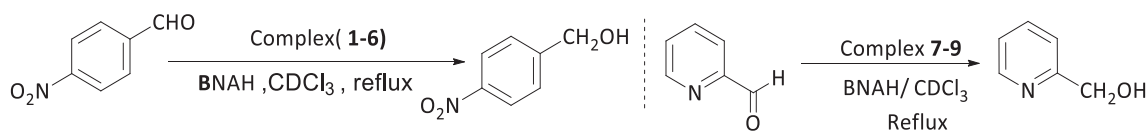
horse LADH. These complexes also react with BNAH to reduce electron-poor aldehydes.

The different reaction conditions for the reduction of aldehyde and ketone by Zn-bithione complexes (1–6) are summarized in Table 1. Complex 6 showed the highest activity among all the complexes tested (Entry 7).

Miecznikowski et al. recently investigated Co(II) complexes (10, 11) with SNS pincer ligand [118] as model complexes to mimic Zn active site present in LADH. The synthetic strategy for the preparation of cobalt complexes 10 and 11 is shown in Scheme 3.



Scheme 1. Synthesis of Zn-bisthione complex (1–6).



Scheme 2. Reduction of aldehyde in presence of Zn-bisthione complexes.

**Table 1**  
Reactivity data of complex 1–6.

Entry	Zn Complex	Time (h)	Conversion
1.	Bisthione ligand precursor	20	<5
2.	1	20	32
3.	2	20	23
4.	3	20	25
5.	4	20	37
6.	5	20	45
7.	6	20	59
8.	ZnCl <sub>2</sub> (10 eq)	20	42

## 2.2. Fe-SNS complexes

Softer donor atoms in ligands are desirable for meridional-binding and mimicking enzymes [120]. Sulfur-nitrogen-based ligands (MeSNS) (see Scheme 4) offer a platform for mimicking models such as Hydrogenases [121], Nitrile hydratases [122], and other oxygen-atom transfer enzymes [123]. The reduction of dinitrogen to ammonia in the biological system is catalyzed by Nitrogenase and iron complexes containing N- and S- donor ligands. Iron complexes containing N- and S-donor

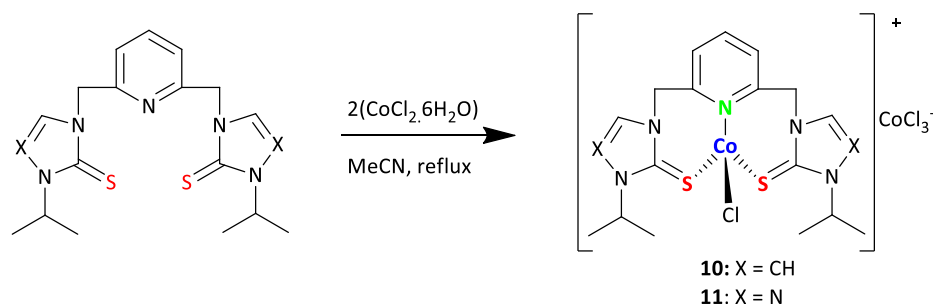
ligands with thiolate and thioamide units show redox activity similar to the biological catalyst. Sulfur-bridged dinuclear iron clusters have an active site similar to metalloenzymes such as Nitrogenase, Catechol dioxygenase [46].

Iron(II), on reaction with multi-donor ligands, afforded a series of mono-, di and tri-nuclear thiolato-bridged Fe(II) complexes (12–16) (Chart 2). These complexes behave as metalloenzymes and offer a platform to mimic many enzymes [124].

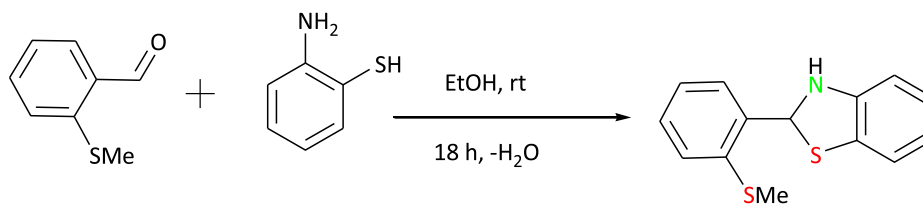
The treatment of (2-methylthiophenyl)benzothiazolidine with Fe(OTf)<sub>2</sub> in the presence of base afforded a trinuclear iron complex, [Fe<sub>3</sub>(μ<sup>2</sup>-SMENS)<sub>4</sub>](OTf)<sub>2</sub> (13). The complex 13 reacts with excess PMePh<sub>2</sub>, CN, and P(OMe)<sub>3</sub> in CH<sub>3</sub>CN to form dinuclear Fe(II) complexes (14–16). The addition of excess P(OMe)<sub>3</sub> to complex 13 in CH<sub>2</sub>Cl<sub>2</sub> produces mononuclear Fe(II) complex, {Fe(MeSNS)[P(OMe)<sub>3</sub>]<sub>3</sub>}(OTf) (12). The synthesis of these complexes (12–16) is demonstrated in Scheme 5.

## 2.3. Copper-SNS complexes

Copper-containing blue proteins are well known as electron transport agents. Small-molecule have been thoroughly investigated for a decent understanding of the inner coordination geometry of copper



Scheme 3. Synthetic scheme of Co-SNS bisthione complexes 10 and 11.



**Scheme 4.** Synthesis of 2-(2-methylthiophenyl)benzothiazolidine (MeSNS).

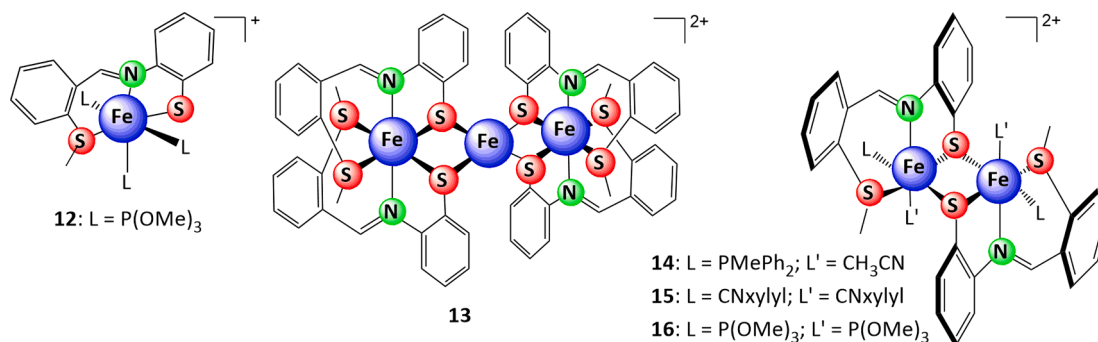
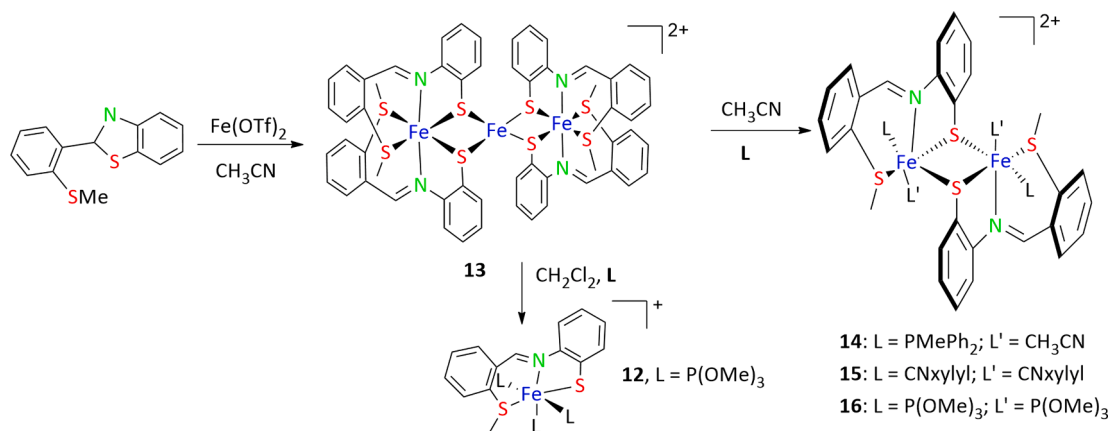


**Chart 2.** Fe-thiolate complexes to mimic different enzymes.



**Scheme 5.** Synthesis of mono-, di-, and tri-nuclear thiolate-Fe complex.

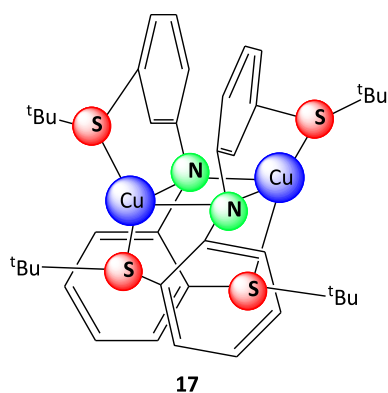


**Chart 3.** The diamond core structure of the Cu-SNS complex.

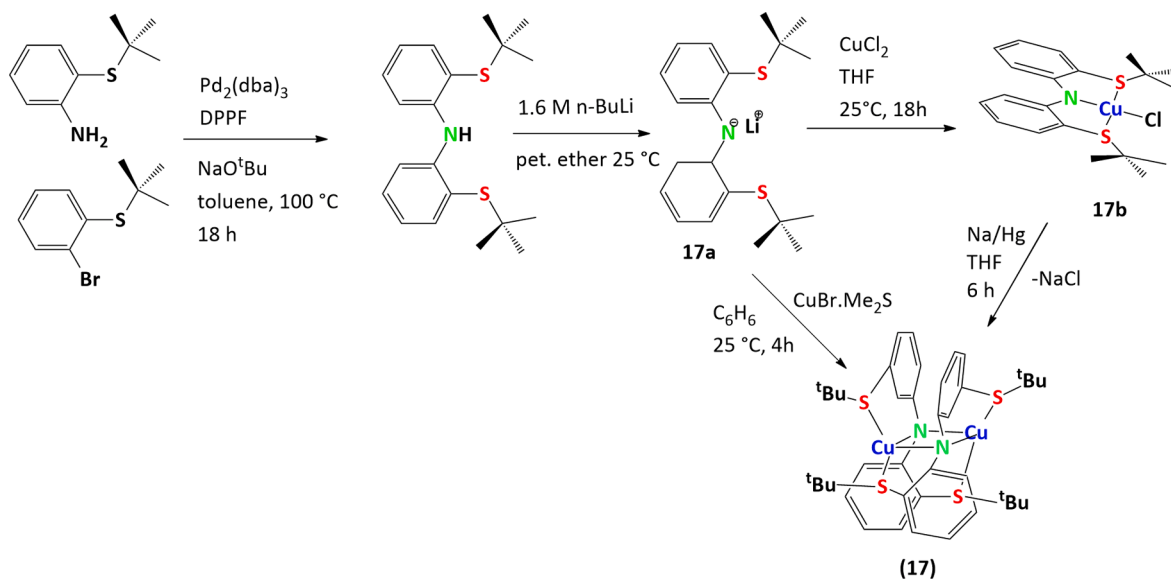
which can provide the mechanism for fast electron transfer [47].

While the variables that affect electron transfer rates in copper proteins are still a subject of conflict, the dinuclear  $\text{Cu}^{2+}$  complex  $[(\text{SNSCu})_2]$  (17) which mimic the activity of Cytochrome C oxidase has been synthesized by incorporating a redox-active Cu having a mixed-valence state with a diamond central core (Chart 3). This complex showed increased electron transfer (ET) into and out of a subsurface of the CuA site and mimics the Cytochrome C oxidase [44].

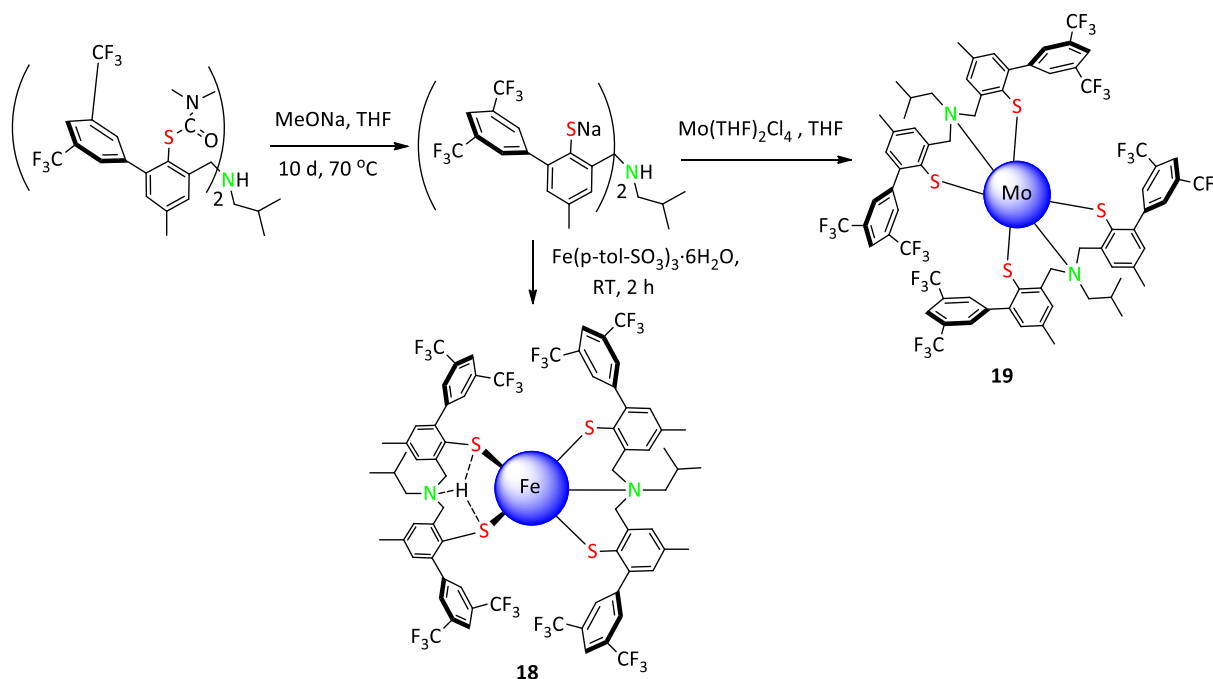
The diamond core Cu complex is synthesized (Scheme 6) by the reaction of  $\text{BrCuSMe}_2$  with lithium salt of SNS in benzene (17). This complex could also be synthesized stoichiometric reduction of 17b with Na/Hg in tetrahydrofuran.

#### 2.4. Iron and molybdenum complexes

Iron (18) and molybdenum (19) complexes have also been synthesized (see Scheme 7) by using pincer-type dianionic  $[\text{NS}_2]^{2-}$  donor ligands. The complex  $[(\text{NS}_2)_2\text{Mo(IV)}]$  (19) has been found suitable for the



Scheme 6. Synthesis of diamond core Cu-SNS complex.



Scheme 7. Synthesis of Mo and Fe-SNS complexes.

oxidation of methanol and isopropanol to formaldehyde and acetone respectively.

The DFT investigations and frontier orbitals analysis indicates that the sulfur donors of the pincer ligand are likely to promote the redox reactions in these complexes. The findings suggest that the  $\text{NS}^{2-}$  ligand is a potential candidate for the design of metal complexes that can be used in biologically inspired sulfur-rich surroundings for effective electron transfer [39].

### 2.5. Nickel and zinc as model complexes

Nickel is an essential component of eight metalloenzymes involved in energy and nitrogen metabolism. The function of redox-active nickel-containing metalloenzyme is to catalyze a redox process, and hence the

reduction potential of nickel is of great importance. Methyl coenzyme M Reductase / Hydrogenase [36,37,125] and thioamide-based organometallic nickel pincer **20** (Chart 5) contain an active site just similar to Lactate Racemase (LarA) [34,109,126] and Nitrogenase have been reported. A butterfly-type structure is observed in the Ni complex **21**. The SNS ligand in **21** is synthesized by the Schiff base condensation of phenyl thiosemicarbazide with 2,2'-dithiodibenzaldehyde (DTDB). The reaction of SNS-ligand with Ni(II) salt results in dimeric Ni(II) complex in which both nickel atoms have an  $\text{NS}_3$  coordination environment. This shows structure relevance to the enzyme and may utilize as an artificial enzyme [35]. Dinionic  $\text{NS}^{2-}$  ligand with  $\text{Zn}^{2+}$  and  $\text{Ni}^{2+}$  provides redox-active complexes **22** and **23** respectively. Complex **23** shows two-electron reduction and oxidation leading to the putative  $\text{Ni}^{3+} / \text{Ni}^+$  and provides electronic plasticity and activity similar to Hydrogenase

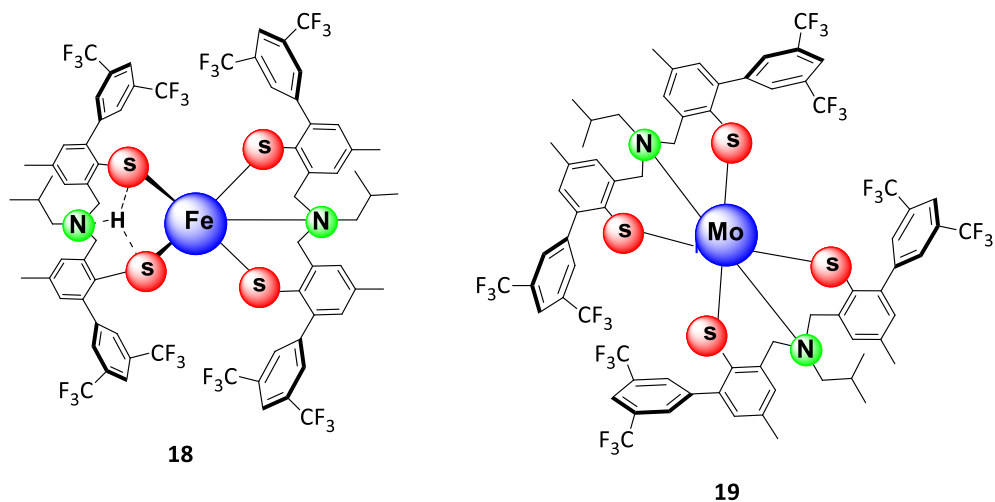


Chart 4. Mo and Fe-SNS complex as model complex for enzyme mimicking.

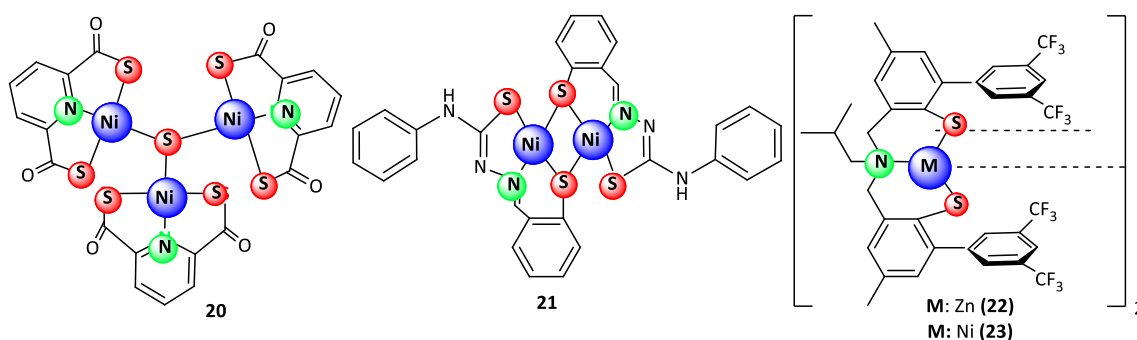
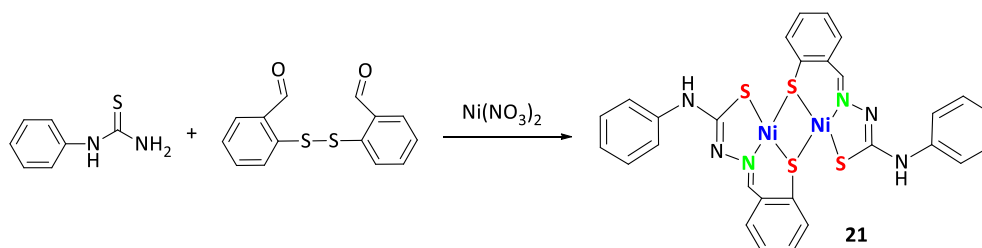


Chart 5. Ni/Zn-SNS as model complexes.



Scheme 8. Synthesis of Ni-thiosemicarbazide complex.

[38].

This dinuclear Ni(II) complex of SNS ligand has been synthesized by the reaction of DTDB with phenylthiosemicarbazone (Scheme 8). An NS3 coordination environment has been observed in complex 21 which is further used as a model complex for nickel-containing metalloenzyme.

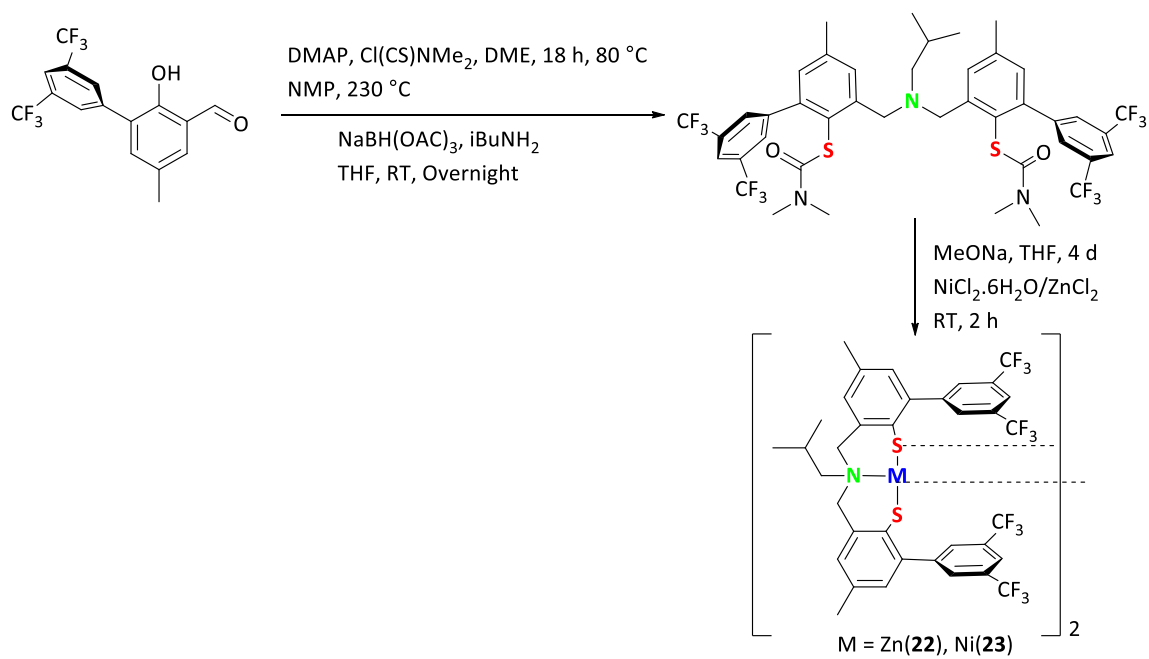
Complexes 22 and 23 have been derived from pincer type NS<sup>2-</sup> ligand. The NS<sup>2-</sup> ligand provides electronic plasticity which is evidenced as 23 showed reversible two-electron oxidation and reduction, leading to the putative Ni<sup>3+</sup>/Ni<sup>3+</sup> and Ni<sup>+</sup>/Ni<sup>+</sup> states. Pincer-type NS<sup>2-</sup> ligand displays significant geometric flexibility and can accommodate different metal ions such as d<sup>7</sup> (Ni<sup>3+</sup>) to d<sup>10</sup> (Zn<sup>2+</sup>) configuration (Scheme 9). Hydrogenase activity is shown by the complex 23, which imparts geometric flexibility due to the methylene connectors between the central amine and the thiophenol groups [38].

## 2.6. [NiFe] hydrogenases model complexes

A bioinspired model to mimic the active site of [NiFe] Hydrogenases, two nickel complexes 24 and 25 supported by tridentate NS<sup>2-</sup> ligands have been synthesized (Chart 6). This model holds a dimeric chemical structure. Theoretical investigations show that the closeness of the Ni(II) ions in the bent complexes favors a weak contact between both the metal centers, which seems to be essential for electrocatalytic proton reduction. These complexes 24 and 25 have been synthesized as given in Scheme 10 [127].

## 3. Photophysical property of SNS complex

Metal complexes have been intensively investigated for their



Scheme 9. Synthesis of Ni and Zn-SNS complex for enzyme mimicking.

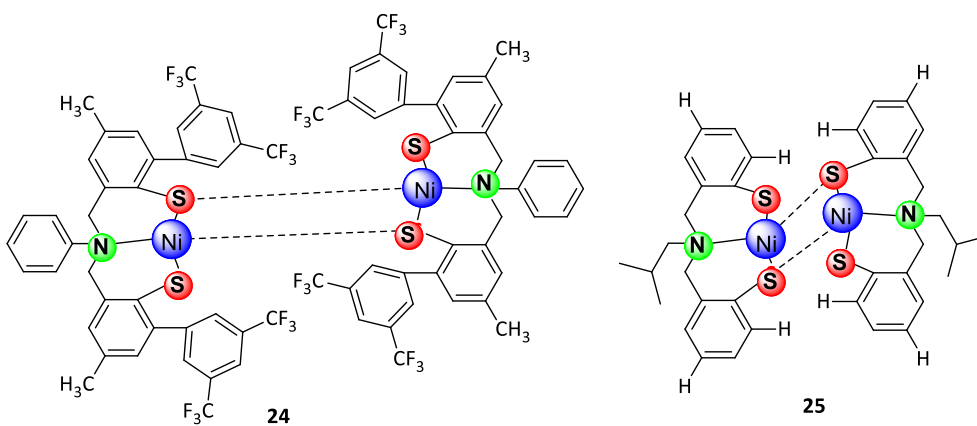
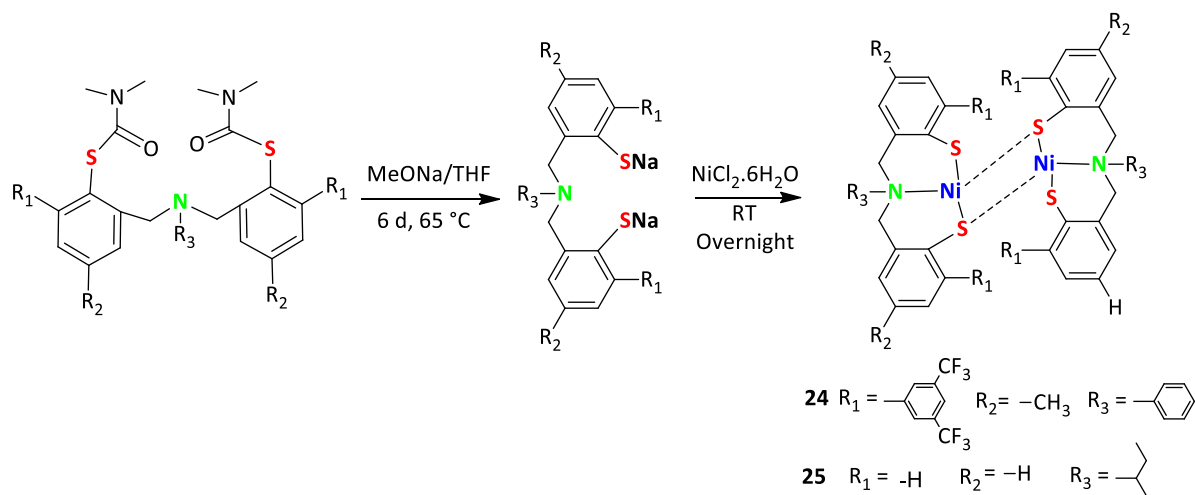
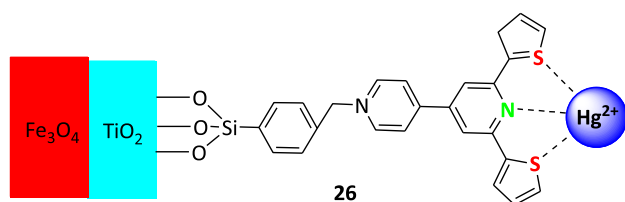


Chart 6. Nickel model complex to mimic NiFe Hydrogenase.



Scheme 10. Synthesis of Ni complexes **24** and **25**.



**Chart 7.** 2,6-Di(thiophene-2-yl)-4,4'-bipyridine immobilized on the  $\text{TiO}_2/\text{Fe}_3\text{O}_4$ .

photochromic and fluorescence behavior [128]. A diverse family of photosensitive compounds has been discovered for their applications in optical and non-optical sensing materials and technologies for the future. Chemosensors detect a wide range of substances and targets, and their detection ability depends on light, pH, temperature, electrical potential, solvent etc. These sensors respond to several chemicals, biological, and physical stimuli [129]. Functional conjugated polymers (CPs) have a wide range of applications, including solar cells, light-emitting diodes, and optical displays etc. SNS conjugated polymer has applications in both chemosensing and other optical devices due to their light-emitting and switching ability. Novel photo- and electro-active

hybrid polymers containing dithienylpyrrole (SNS) [130–132] were synthesized and electrochemically polymerized [133,134]. Their optical properties were predetermined using computational study [134]. Structural and electrochemical studies suggest that the SNS maintains redox properties which are probably due to increased metal–ligand covalency. Tungsten complex  $[\text{W}(\text{SNS})_2]$  acts as a redox-active metal-ligand, and other bimetallic complexes with Ni, Pt, and Pd display redox processes [135–137]. It is reported that molybdenum and tungsten complexes with dianionic tridentate pincer-type ligands  $[\text{W}(\text{SEtN}(\text{Me})\text{EtS})_2]$  and  $[\text{Mo}(\text{SEtN}(\text{Me}))_2]$  exhibit high volatility and a clean thermal breakdown [56]. The Pd- and Rh-SNS complexes have been studied for their electrochemical properties, such as the inhibition of the hydrogen evolution process (HER). Incorporation of a  $\text{Na}^+$  or  $\text{Ba}^{2+}$  ion into the azacrown has been found to increase the overpotential for hydrogen evolution [138]. Further research into redox behavior and electrochemistry are encouraged by this finding. It has been observed that such complexes can act as chemosensors due to their remarkable chelation properties and binding ability due to mixed donor atom chelation. Some of the important applications of SNS conjugated polymers are listed in the following subsections.

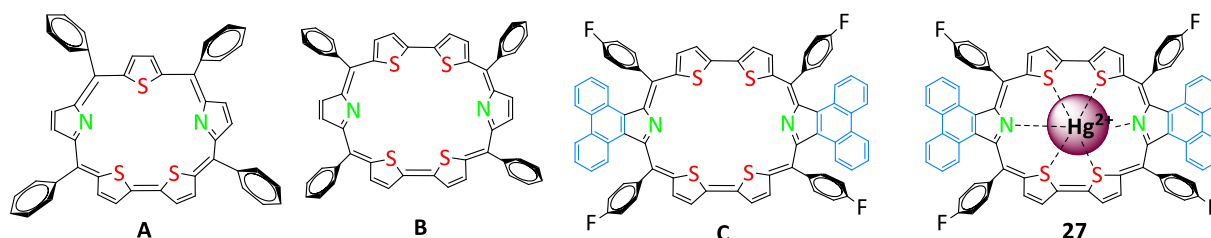


**Chart 8.** Porphyrin derived systems for several applications.

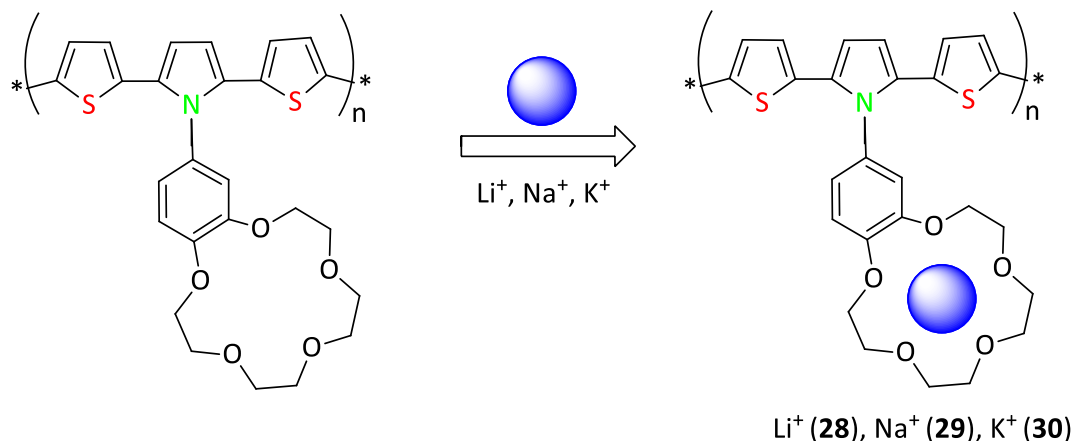


**Chart 9.** The polymer of benzo-15-crown-5 for the detection of  $\text{Li}^+$ ,  $\text{Na}^+$  and  $\text{K}^+$  ions.

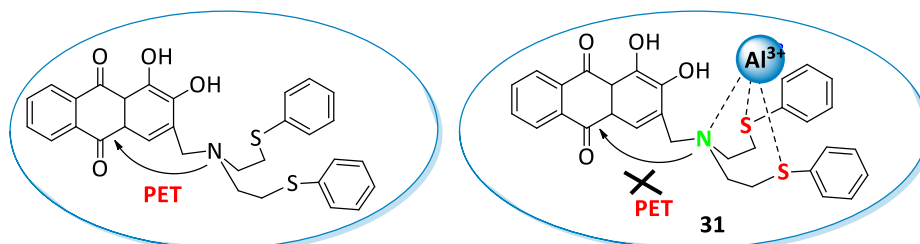


**Chart 10.** Detection of  $\text{Al}^{3+}$  via inhibition of PET.

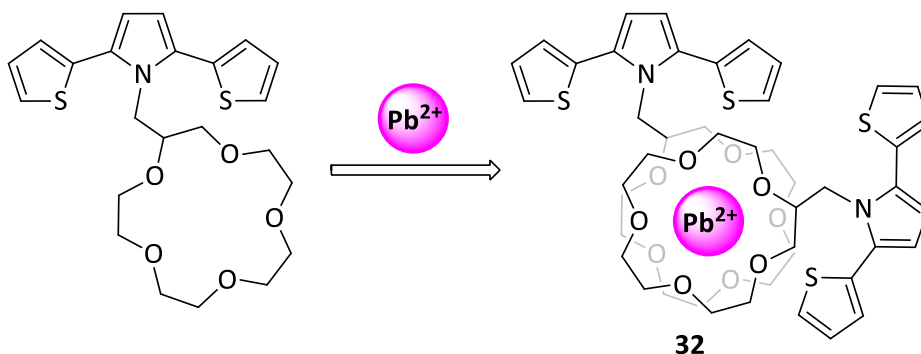


Chart 11. 2,5-Di(thien-2-yl)pyrrole-(15-crown-5) scaffold for  $\text{Pb}^{2+}$  detection.

### 3.1. Chemosensor

SNS ligands have been successfully employed as chemosensors to detect various cation/anion and other target substances such as glucose. The interaction of three donors with a cation/anion or molecule results in the formation of one or two chelate rings, which is responsible for their detection. Poly-SNS are also useful for detection and their chemosensing properties are discussed in the following subsections.

#### 3.1.1. $\text{Hg}^{2+}$ detection

Mercury ions ( $\text{Hg}^{2+}$ ), a serious poisonous hazard, have toxic effects on humans and other living organisms [139,140]. Various methods have been reported to detect  $\text{Hg}^{2+}$  ions but suffer from limitations like the requirement of bulky and expensive equipment [141]. Thus, a more convenient way such as optical or electrochemical method is required for detection and removal of  $\text{Hg}^{2+}$  ions. In this regard, Zn(II), Cd(II), and Hg(II) complexes  $[\text{M}(\text{L})_2(\text{ClO}_4)_2]$  of ligand  $[\text{L} = 2,6\text{-bis}(\text{methylthiomethyl})\text{pyridine}]$  have been synthesized and studied for exchange rates. The relative intermolecular ligand-exchange rates of the complexes follow the order  $\text{Cd}(\text{II}) > \text{Zn}(\text{II}) > \text{Hg}(\text{II})$ . This suggests that the toxicity of Hg(II) is due to the strong interaction of mercury ions with SNS ligand [142]. SNS-ligated systems such as 2,6-di(thiophene-2-yl)-4,4'-bipyridine have been reported as a good chelator for  $\text{Hg}^{2+}$  ions due to the presence of two sulfur and a chelating environment. The fluorescence emission method has been used to detect  $\text{Hg}^{2+}$  ions and turn off and turn on bands observed at 413 and 563 nm, respectively, which has also been confirmed by computational analysis. Furthermore, covalent immobilization of this ligand on surface-enhanced nanostructures  $\text{TiO}_2/\text{Fe}_3\text{O}_4$  (Chart 7), generates a novel material 26 for efficient mercury uptake [143].

Porphyrin-derived systems having different donor atoms have been used for photo-optical properties and as a chemosensor for the detection of the target molecule. They have been studied for various applications as devices and switches (A–C) (Chart 8) and also studied for their photochemical properties [144–150].

Polyurethane membrane having ring 'C' has been used to make test strips for  $\text{Hg}^{2+}$  screening. This strip showed an unusual bathochromic shift which results in an absorption spectrum that corresponds to solar energy. A yellow (594 nm) and a red (633 nm) He-Ne laser have been used to examine the ratiometric response [151]. The mercury ion has been found to fit in the cavity of 'C' due to its strong interaction with sulfur atoms (27).

#### 3.1.2. Alkali metal detection

The polymer of benzo-15-crown-5 (SNS-crown) has been reported for the detection of alkali metals. Highly selective, clear, and reversible voltammetric responses of the conjugated polymer (PSNS-crown) film towards the alkali such as  $\text{Li}^+$ ,  $\text{Na}^+$ , and  $\text{K}^+$  has been observed. The benzo-15-crown-5 cavity has been responsible for the binding of these metal ions. The metals can easily be introduced into cavities and fit well

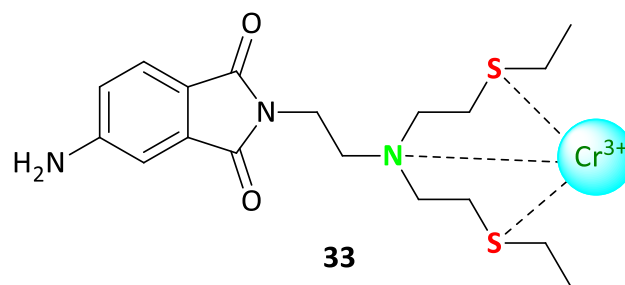


Chart 12. Detection of  $\text{Cr}^{3+}$  by SNS donor ligand.

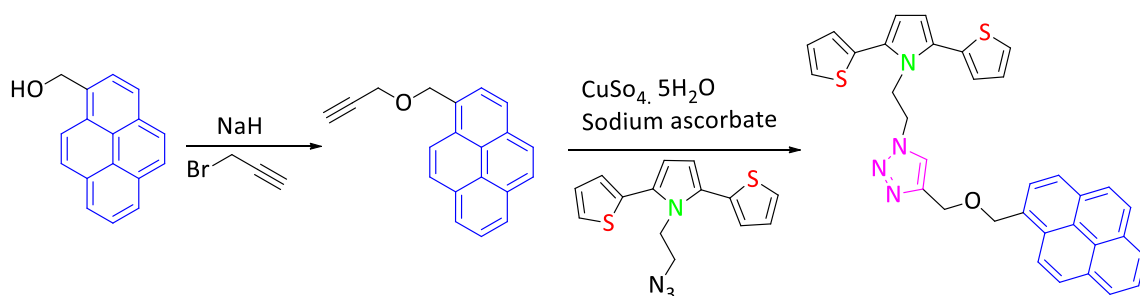
due to the strong interaction with oxygen (28–30; Chart 9) [77].

#### 3.1.3. $\text{Al}^{3+}$ detection

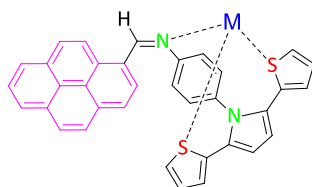
$\text{Al}^{3+}$  is also categorized as toxic metal to the living organism and environment and may cause several severe ailments such as Alzheimer's disease and osteoporosis [152]. Hence the development of sensors to detect  $\text{Al}^{3+}$  ions is highly important. The photo-induced electron transfer (PET) process senses both cations as well as anions. S-donor present in the ligand framework inhibits the PET process, and N-donor stimulates. Thus, both are responsible for the fluorescent ON-OFF operation. A chemosensor has been synthesized by using conjugated  $\text{S}_2\text{N}$  moiety as a chelating agent and 1,2-dihydroxyanthraquinone as a fluorophore. This chemosensor exhibits excellent turn-off fluorescence signal in presence of  $\text{Al}^{3+}$  allowing its reversible detection in presence of a wide range of competing metal ions and anions.  $\text{Al}^{3+}$  is chelated by SNS ligand and forms a chelate complex 31, responsible for inhibiting PET's process which results in fast detection (Chart 10) [153].

#### 3.1.4. $\text{Pb}^{2+}$ detection

$\text{Pb}^{2+}$  has significant physicochemical characteristics which have been traced back in ancient times. Its significance cannot be overlooked due to key qualities like softness, elasticity, rigidity, weak conductance, and corrosion resistance, yet it is generally acknowledged for its poisonous action.  $\text{Pb}^{2+}$  is non-biodegradable therefore persists in the environment [154]. It mostly causes cognitive impairment and diminishes the intelligence quotient (IQ).  $\text{Pb}^{2+}$  ions can cause Anemia which increases the serum pressure and can result in long-term brain damage in both adults and children [155]. For the detection of  $\text{Pb}^{2+}$  ions, Aysun and co-workers reported 2,5-di(thien-2-yl)pyrrole scaffold attached with the 15-crown-5 unit (32). This compound consists of an SNS unit with a pendant crown ether motif. The SNS unit acts as a fluorophore and the 15-crown-5 unit act as a binding site for turn-off fluorimetric recognition of  $\text{Pb}^{2+}$  ion (Chart 11). The fluorescence approach is centered on reductive photoinduced electron transfer [PET] facilitated by cations [63].



Scheme 11. Synthesis of pyrene-SNS ligand.



34 M = Cu<sup>2+</sup>; 35 M = Zn<sup>2+</sup>  
36 M = Cd<sup>2+</sup>; 37 M = Fe<sup>3+</sup>

Chart 13. Mode of binding of metal ions with pyrene Schiff base ligand.

### 3.1.5. Cr<sup>3+</sup> ion detection

The fluorescence quenching method has been the most robust and sensitive means of detecting Cr<sup>3+</sup> ions. In this context, Samanta et al. reported an “off-on” fluorescence chemosensor (33) derived from the SNS ligand for the selective and facile detection of Cr(III) ions. Due to the disruption of PET communication between receptor and fluorophore moieties, an approximate 17-fold enhancement in fluorescence intensity

has been observed (Chart 12) [62].

### 3.1.6. Pyrene-SNS system as chemosensor

The pyrene-SNS (PR-SNS) ligands preferentially detect metal ions in toxic samples using adaptive fluorescent and electrochemical techniques. The synthetic strategy for the preparation of such a ligand is shown in Scheme 11. The polymerization of PR-SNS results in the formation of multicromic polymer which could be an ideal candidate for

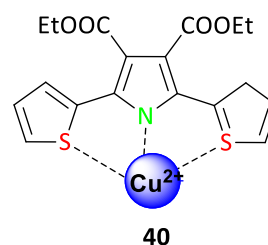
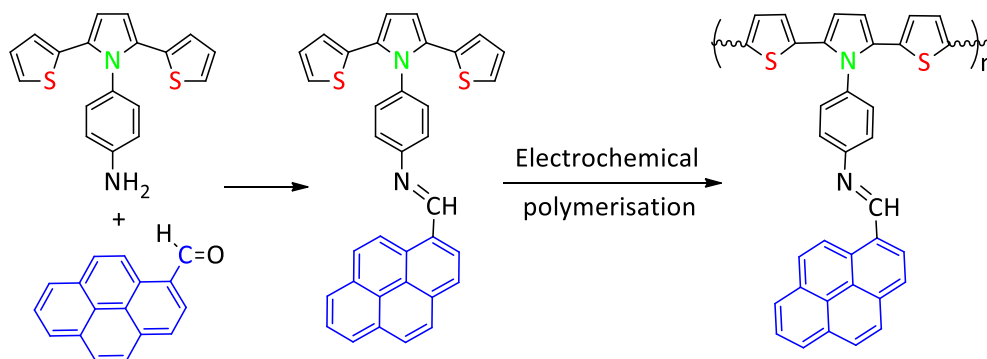


Chart 15. Cu<sup>2+</sup> sensing with SNS donor ligand.



Scheme 12. Preparation of poly(2,5-dithienylpyrrole)-pyrene [P(TPP)] Schiff base sensor for Fe<sup>+3</sup> ions.

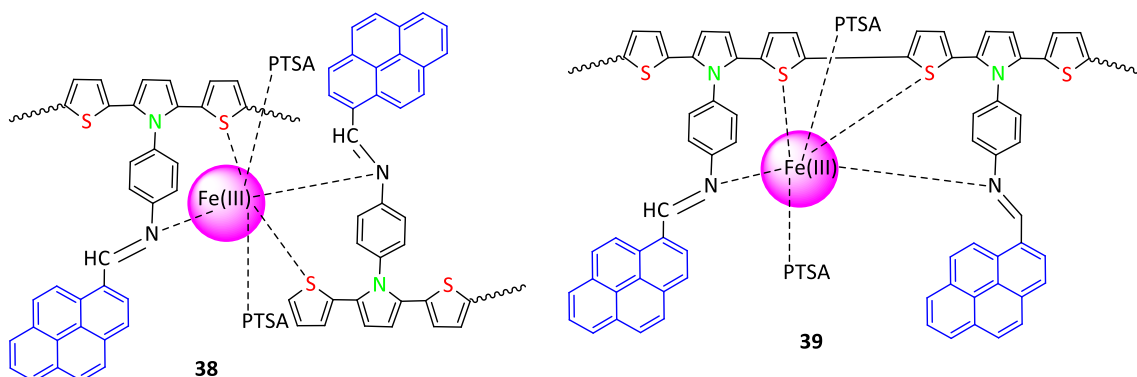
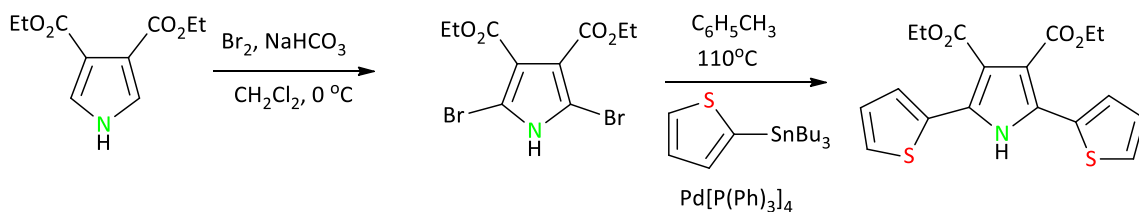
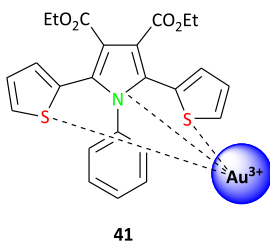


Chart 14. Proposed binding modes of Fe<sup>+3</sup> with P(TPP).



Scheme 13. Synthesis of SNS as Cu(II) sensing probe.

Chart 16. Nonreaction-based fluorescent probe for Au<sup>3+</sup> detection.

display applications [132].

Furthermore, the Schiff base of the pyrene-SNS system has been investigated as a fluorescence probe for the detection of metals ions (Chart 13) [156]. It has been found that this probe is suitable for the sensing of metal ions such as Cu<sup>2+</sup>, Zn<sup>2+</sup>, Cd<sup>2+</sup> and Fe<sup>3+</sup>.

Poly(2,5-dithienylpyrrole)-pyrene Schiff base derivative [P(TPP)] has been synthesized via imine formation followed by electrochemical polymerization (Scheme 12). This sensor has been found suitable for the selective detection of iron(III) ions. P(TPP) has a robust

potentiometric response to Fe(III) ions [157]. However, no significant electrochemical signal has been observed in the presence of other metal ion solutions such as Fe(II), Zn(II), Cu(II), Hg(II), and Cd(II). This sensor demonstrated excellent stability, sensitivity, and reproducibility for the detection of Fe(III) ions and two binding modes of Fe(III) with ligand (38, 39) have been proposed (Chart 14).

### 3.1.7. Cu sensing

A simple, selective and triple channel responsive Cu<sup>2+</sup> probe (40) has been synthesized [158]. This probe consists of an SNS core unit with

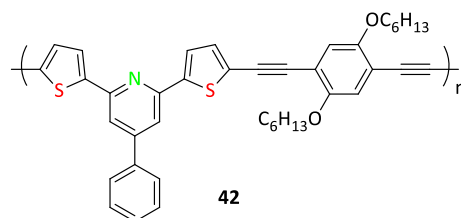
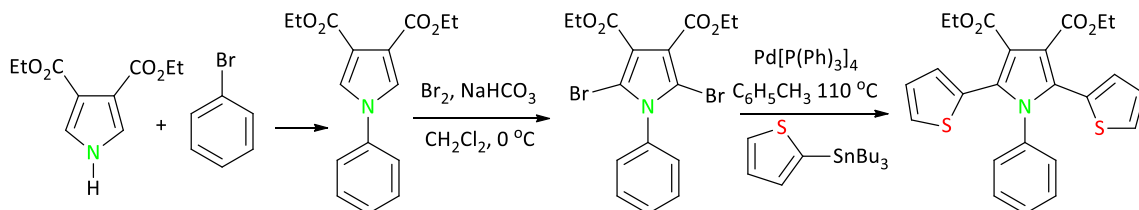
strong electron-withdrawing substituents on the central pyrrole unit (Chart 15). This probe is capable of detecting Cu<sup>2+</sup> ions by calorimetry, fluorimetry, and voltammetry methods. This property makes this ligand very viable for practical applications. The synthesis of this probe is given in Scheme 13.

### 3.1.8. Au<sup>3+</sup> probe

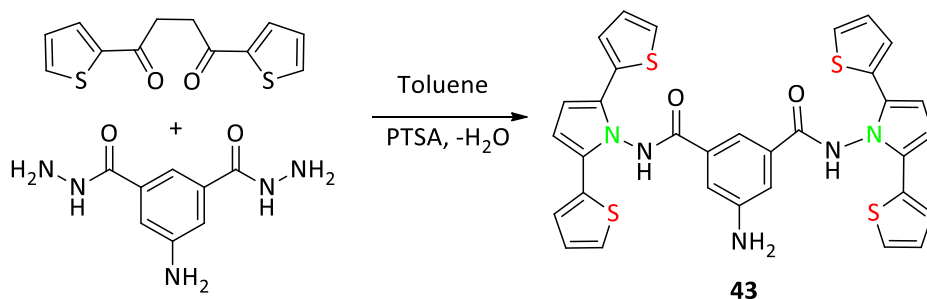
A diethyl-1-phenyl-2,5-di(thiophen-2-yl)-1-*H*-pyrrole-3,4-dicarboxylate has been reported to be a simple, selective, and effective turn-off fluorescent probe for Au<sup>3+</sup> ions (Chart 16). This probe has been reported as the first nonreaction-based fluorescent probe for Au<sup>3+</sup> detection. This probe has strong electron-withdrawing ester substituents on central pyrrole ring. The synthetic methodology is shown by Scheme 14. This is the first example of a fluorescent gold probe paving the path for future research [159].

### 3.1.9. Pd<sup>2+</sup> sensor

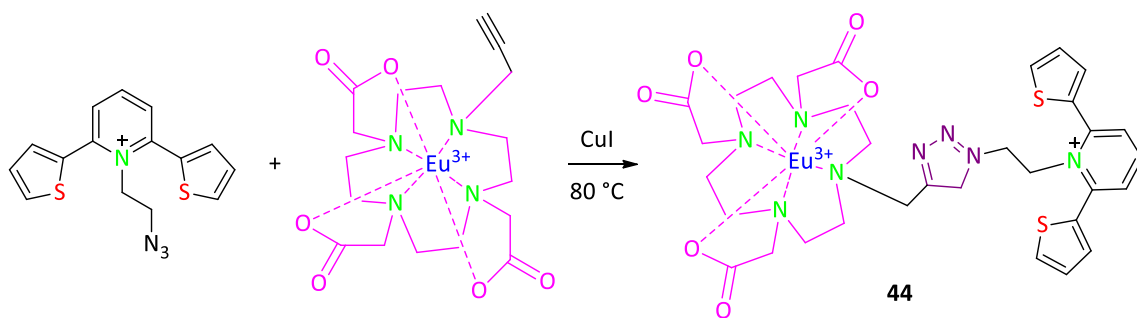
Palladium, a transition metal, is now used in electrical and electronic devices, dental equipment, hydrogen storage, ornaments, and as catalysts. Due to the automotive fuel system, a considerable amount of

Chart 17. A fluorometric Pd<sup>2+</sup> sensor.

Scheme 14. Synthesis of nonreaction-based fluorescent probe.



Scheme 15. Synthesis of BTP.



Scheme 16. Synthesis of fluoride detection system by 1,3-dipolar cycloaddition reaction.

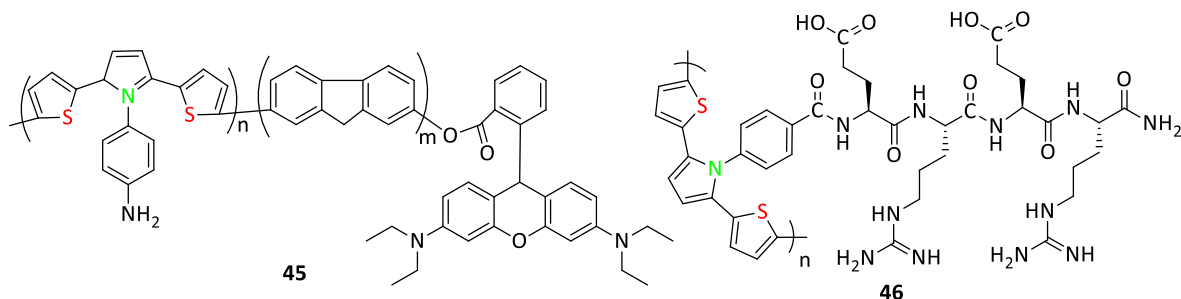


Chart 18. Glucose sensing using receptors 45 and 46.

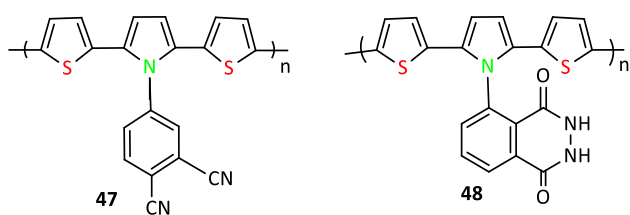


Chart 19. Conjugated polymer PSNS (47), PSNS-Lum (48) as sensors.

palladium is released into the environment, especially with the rapid expansion in the number of vehicles. The most common oxidation states of Pd are; Pd<sup>0</sup> (metallic), Pd<sup>2+</sup> and Pd<sup>4+</sup>. Its metallic form has negligible or little in vitro cytotoxicity; nonetheless, Pd ions can trigger several cytotoxic effects that can cause significant skin and eye irritation. A novel conjugated polymer chemosensor (42) containing 2,6-bis(2-thienyl)pyridine has been synthesized and exhibits high sensitivity and selectivity for palladium ion detection using fluorescent

spectroscopy (Chart 17) [160].

### 3.1.10. BTP as sensor

The monomer 5-amino-N1,N3-bis(2,5-di(thiophen-2-yl)-1H-pyrrol-1-yl)isophthalamide (BTP) has improved optical and electrical properties as compared to 2,5-di(2-thienyl)pyrrole derivative. The introduction of conjugated thienylpyrrole electroactive group and amide substitution into the planar structure, effectively delocalizes the bonds have been observed. This enhances the conductive (optical and electrical) properties of the resulting monomer. Furthermore, the synthesized monomer 43 (BTP) was copolymerized with EDOT using various monomer feed ratios, and the characteristics of the copolymer were compared to the homopolymer [161] Scheme 15.

### 3.1.11. Fluoride sensing

Fluorides are not toxic, but an excess of this anion can cause dental and skeletal problems. Hence, a selective and sensitive detection probe made up of an Eu(III) complex and a 2,5-di(thien-2-yl)pyrrole (SNS)

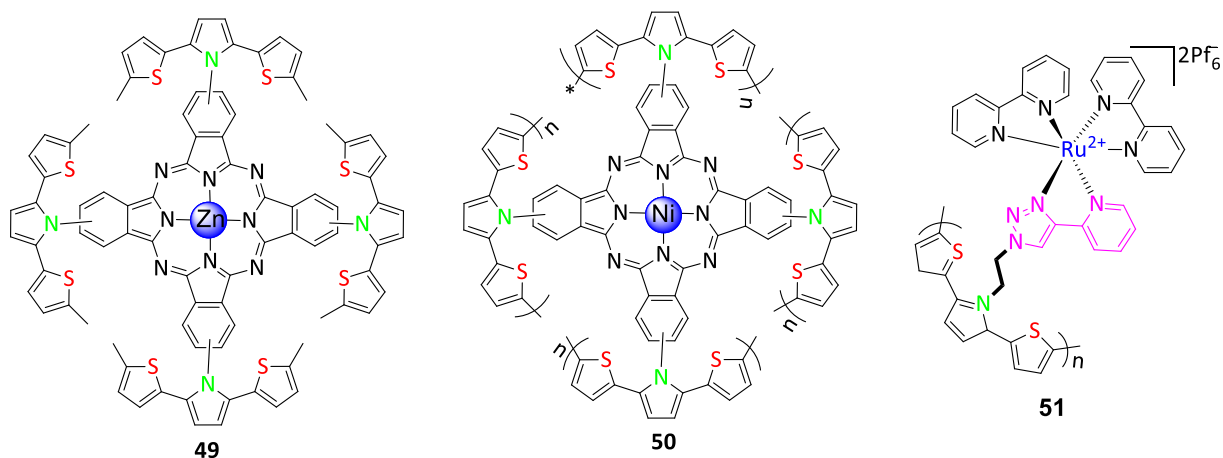


Chart 20. ZnPc-SNS, NiPc-SNS and Ru-BPY-SNS for different applications.

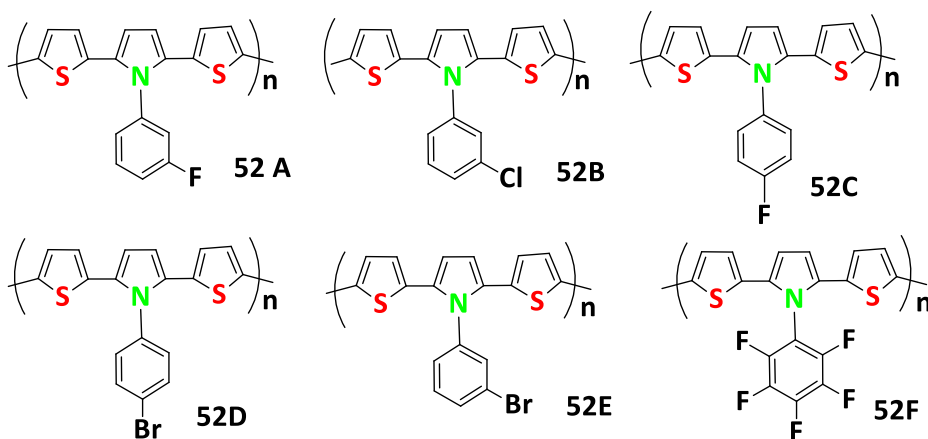


Chart 21. Halo derivatives of poly-SNS suitable for the fabrication of the electrochromic device.

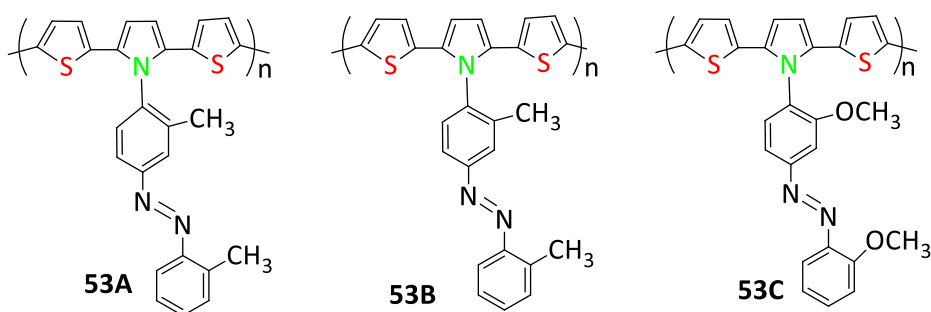


Chart 22. Dithienylpyrroles based azo dyes having photoisomerism properties.

scaffold (**44**) has been synthesized using a Click reaction. This revolutionary material has appeared as a turn-on phosphorescent fluoride probe (Scheme 16). It is the first example of combining an SNS unit with an Eu(III) complex, which can induce a potent luminogenic sensitivity to fluoride ions over other anions [162].

### 3.1.12. Glucose sensing

Copolymerization of a rhodamine-based electrochemically active monomer (RDC) with an SNS monomer (Chart 18) has resulted in **45** which has been utilized as a fluorescence sensor for glucose detection. This sensor utilizes the oxygen associated within the layer of the electrode, which shows fluorescence during glucose-GOx coupling. The glucose concentration was accurately measured ranging from 0.05 to 1

mM. This unique approach can be used for rapid and effective fluorescence sensing of glucose [72].

Another simple and efficient strategy for biosensing of glucose has been achieved using peptide-SNS type polymer (**46**; Chart 18). Solid-phase peptide synthesis was employed to tie the SNS-type monomer with a carboxylic acid functional group to the peptide's C-terminus to produce the peptide-bearing monomers. The peptide-SNS monomer was electrochemically polymerized on the electrode surface in the presence of glucose. The biosensor shows promising feasibility for the quantitative detection of glucose in drinks [163].

### 3.1.13. PSNS-PN, PSNS-Lum conjugated polymer as chemosensor

Electrochemical polymerization of 4-(2,5-di-2-thiophen-2-yl)pyrrol-

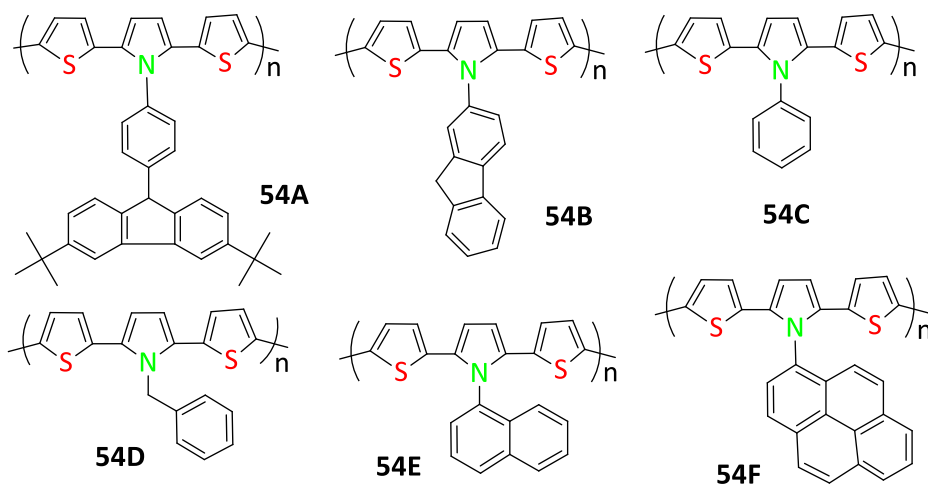
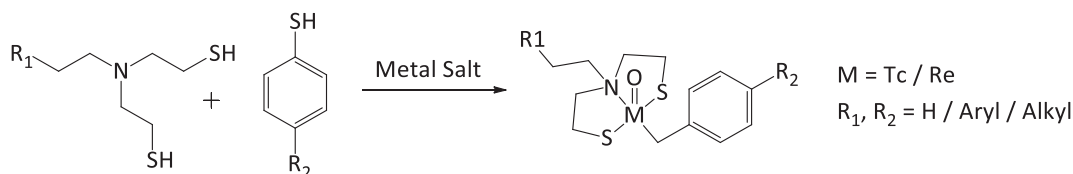


Chart 23. Poly-SNS derivative showing electrochromism.



Scheme 17. General synthetic scheme of oxorhenium / oxotechnetium complexes.

1-yl)-phthalonitrile (SNS-PN) (**47**; Chart 19) resulted in the formation of a novel conducting polymer. The switching ability of polymer has also been examined. It has been found that the fluorescence intensity of SNS-PN increases in the presence of cations. SNS-Lum (**48**), a diverse-stimuli sensitive chemiluminescent system (Chart 19) has also been synthesized. It is the first example of conjugated polymers containing luminol arms and produces chemiluminescence in the presence of a superoxide radical anion. It has a unique application in forensic science for the detection of bloodstains. It has also been found suitable for the detection of  $\text{Cu}^{2+}$  and  $\text{Fe}^{3+}$  ions [80].

### 3.2. Organic laser/LED/switches/devices

Metal complexes have been widely investigated for their optoelectric properties such as light-emitting diodes and lasers [164-166]. Electrochromism is an important phenomenon that occurs in metal complexes for the reversible color change in the visible region. It operates at low voltage and has long-term switching stability, high contrast ratio, and coloration efficiency [167,168]. Such systems showed switching on-off behavior of oxidized and reduced states upon an applied electric potential [169-171]. The nucleation and growth processes of the polymer as well as its use as a *p*-layer in photocells have been studied using chronoamperometry [172].

The zinc phthalocyanine (ZnPc-SNS; **49**) and nickel phthalocyanine (NiPc-SNS; **50**) have been synthesized and utilized in optical devices (Chart 20). Fluorescence observations indicate that ZnPc-SNS is a robust blue and orange light emitter with possible advantages in organic lasers and/or LEDs [73]. The NiPc-SNS film can be reversibly cycled and exhibits electrochromic behavior having a dark olive green and dark blue color in the neutral and oxidized state respectively [74].

A Ru(II) complex (**51**; Ru-BPY-SNS) of polymerizable thiophene anchored on pyridine-triazole ligand via alkyl spacer has been synthesized (Chart 20). This complex was successfully electropolymerized and exhibits multiple reversible redox behavior. It has been observed that anchoring the Ru complex to PSNS improved its coloring performance via a reversible modulation of strong MLCT following polymer oxidation in the visible region. The cathodic activity was controlled by the Ru center while the anodic behavior was influenced by both the conjugated backbone and the Ru center. Following the successive anodic and cathodic polarisation, the polymers showed red legs of RGB [130].

Halogen derivatives (**52A-52F**) of polythionylpyrrole are shown in Chart 21. The SNS derivatives, P(*m*-FPTP) **52A**, P(*m*-ClPTP) **52B**, P(*m*-FPTP) **52C**, and P(*p*-BrPTP) **52D**, were prepared and the substituent

effect has been studied by electrochemical method. It has been observed that P(*m*-FPTP) has the highest optical contrast value with a reasonably rapid switching time [82]. Another polymerized *meta*-bromo derivative (*m*-BrPTP) **52C** has emerged as a dual-type electrochromic device (ECD) which switches between yellow and blue [83]. A per-fluoro derivative FPTPy (**52F**) has also been found suitable for the formation of dual-type electrochromic devices having good switching times, contrast value and optical memories [84] (see Chart 21).

Dithienylpyrroles based azo dyes and their polymers (**53A-53C**) have been synthesized and exhibits photoisomerism Chart 22. The **53B** showed a color change from yellowish green to dark green, whereas **53C** showed a color change from mustard to green [75].

Several other dithienylpyrroles based polymers of fluorine, carbazole, naphthyl, pyrene etc. (**54A-54F**) has been reported (Chart 23). The fluorescent polymer PSNSF (**54A**) based on fluorene was exhibited high coloration efficiency (CE), high redox stability and very low response time [79]. Another carbazole-based polymer **54B** switches among three different colors (orange, green, and blue) [173]. The film of polymer **54C** and [174] polymer **54D** has emerged as efficient electrochromic agents with good switching capabilities and optical memory [175]. Polymer **54E** showed stable electrochromic behavior in a neutral state (yellow) then green and violet in the oxidized state. Although the monomer of **54E** is almost nonfluorescent but its polymer is a yellow and/or green light emitter [76]. A new hybrid compound of pyrene derivative (**54F**) exhibits both fluorescent and multi-electrochromic properties. Upon oxidation, the polymer showed several changes from yellowish orange to greenish-yellow to green/blue to blue [176].

## 4. SNS ligated system as bioimaging agents

The oxo-rhenium and oxo-technetium complexes of SNS ligand offer a major benefit in the diagnostic arena as a labeling agent for tumor cells and brain cells [101]. SNS-based nuclear medicine containing trace metals  $^{99\text{m}}\text{Tc}$  and  $^{186/188}\text{Re}$  have been identified as a labeling agent for brain cell dopamine [104] and serotonin [177]. These complexes cross BBB (Blood Brain Barrier) and are observed by single-photon emission computed tomography (SPECT) or positron emission tomography (PET) [178]. Cytotoxicity is measured in terms of  $\text{IC}_{50}$  value and psychiatric activity is examined by brain uptake and retention time. These complexes are susceptible to liposomes for the absorption of drugs [179]. For the construction of the imaging agent, three structural units are used: metal core, chelator, and receptor (Fig. 4). Metal-core is oxo-nitro-rhenium / oxo-nitrido-technetium chelated with SNS unit and

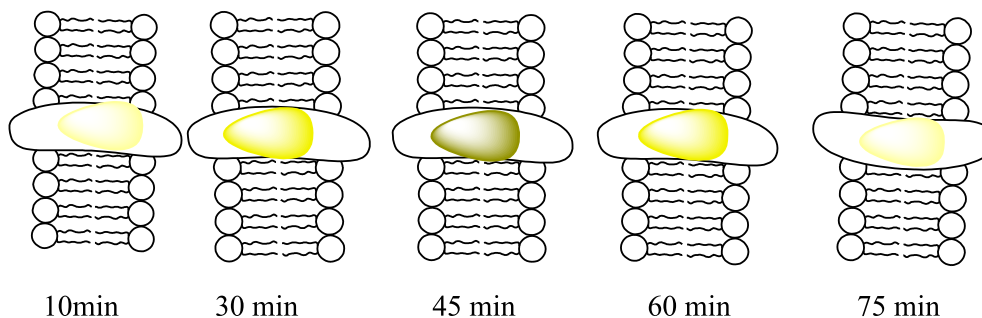


Fig. 5. Pictorial representation of bioimaging by  $^{99\text{m}}\text{Tc}$  /  $^{186/188}\text{Re}$ -SNS complex in brain / tumor cell.

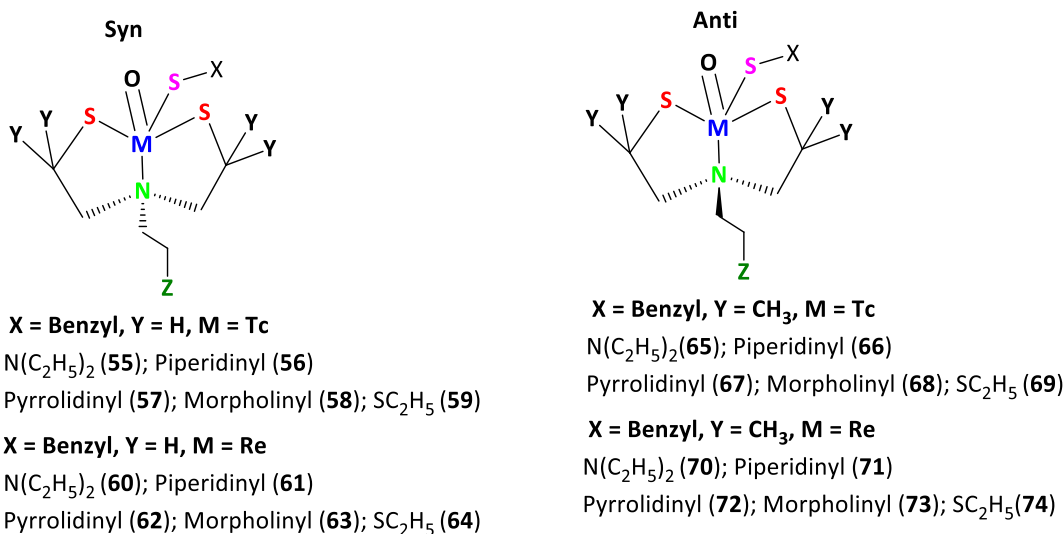


Chart 24. Syn and anti-complex of oxorhenium and oxotechnetium.

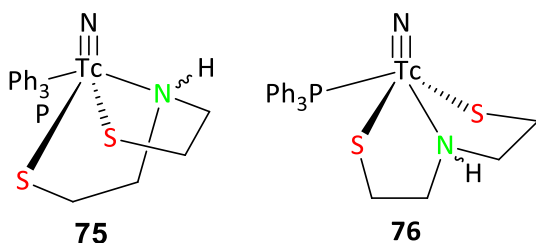


Chart 25. SNS/P nitrido complex of Tc.

contains a monodentate or bidentate receptor and a lipophilic or neutral pharmacological unit. The tridentate SNS ligand with a variable substituent on the N atom can alter the activity of the resulting complexes [94]. The steps involved in the synthesis of such imaging agents are shown in Scheme 17.

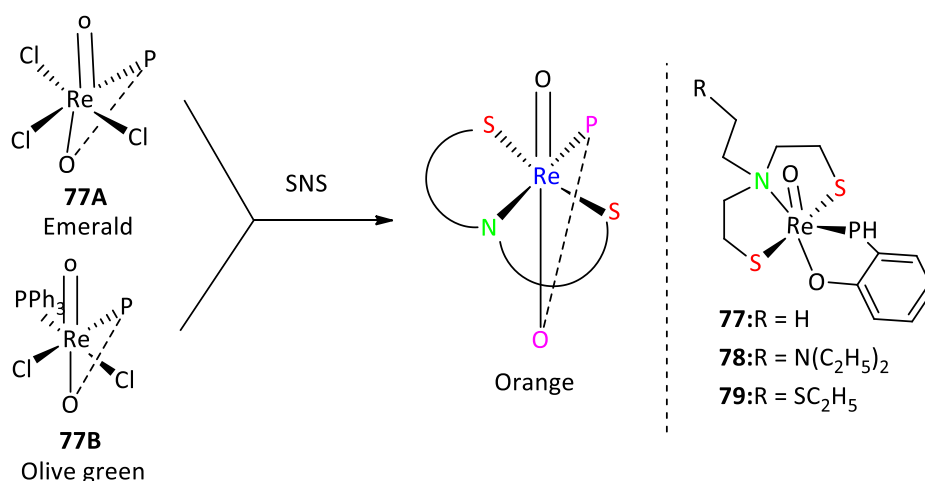
Regional cerebral blood flow (rCBF) is a critical parameter in the diagnosis of a wide range of cerebrovascular and neurological conditions and other mental disorders. For such application, complex design is critical since the complex should not cross the blood–brain barrier more than the required limit and a limited amount of complex must be used for imaging. Several tetradentate chelating systems, such as the  $N_2S_2$  or the  $N_4$  donor atom set, have previously been reported to form neutral

and lipophilic complexes with  $^{99m}Tc$  [89]. Very few of them such as  $^{99m}Tc$ -d,l-HMPAO and  $^{99m}Tc$ -ECD have been accepted for clinical trials. However, none of them are effective due to their instability. The variation in concentration with the time of such complexes is depicted in Fig. 5.

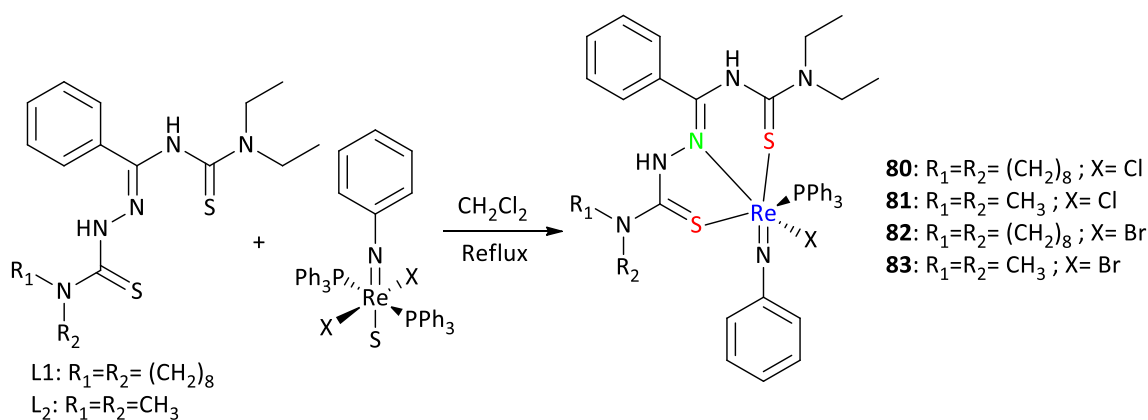
To overcome the instability of tetradentate ligated complexes, tridentate moiety with a receptor has been tested. Various tridentate chelator ligands containing sulfur, nitrogen and oxygen are ONO, ONS, SSS, SOS, SNS or SNN have been examined. Furthermore, a monoanionic monodentate thiolato (R-S) coligand on a suitable  $TcO^{3+}$  precursor has also been designed for imaging purposes. Although oxometal core is commonly utilized for imaging purposes, nitrido complexes have also been tested [180]. Generally, coligand is substituted sulfur (R-S) but other coligand such as monodentate phosphorous and other bidentate systems has also been explored.

#### 4.1. Mixed ligand approach (SNS/S, SNS/P, SNS/PO)

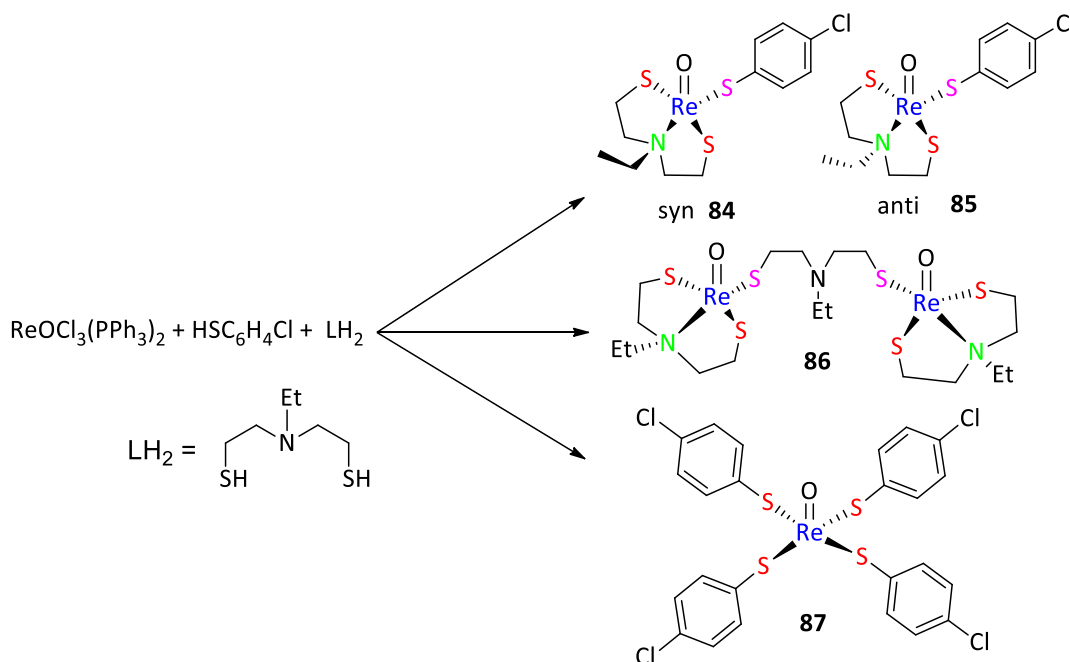
The findings indicate that mixed ligand systems can be used to generate target-specific radiopharmaceuticals ( $^{186}Re / ^{99m}Tc / ^{188}Re$ ) for therapeutic applications. Several investigations have been conducted to determine the effect of different substituents. These are classified according to the receptor pharmacological unit, which is interchangeable. There should be a perfect combination of substituents on SNS and



Scheme 18. Synthesis of SNS/PO complex of oxorhenium.



Scheme 19. Synthesis of (3 + 2) thiosemicarbazone complexes.

Scheme 20. The effect of variation of metal:HSC<sub>6</sub>H<sub>4</sub>Cl:H<sub>2</sub>L ratio.

coligand so that they can't penetrate the blood brain barrier. Few of the systems are described in subsections.

#### 4.1.1. 3 + 1 system

The oxo-rhenium or oxo-technetium chelated with an SNS unit in addition to a monodentate ligand such as  $RS^-$  has been synthesized by Papadopoulos and coworkers (Scheme 17). The ratio of ligand, receptor, metal, and reaction conditions plays a significant role in the synthesis of such complexes [181]. Papadopoulos et al. synthesized both syn and anti isomer of oxorhenium and oxotechnetium complexes (55–74; Chart 24) with varying groups on central N atom. These complexes showed fluxional behavior but the tendency of oxorhenium complexes are greater than oxotechnetium complexes. The ratio of syn- to anti-isomer has been found to be 25:1. Syn isomers showed more activity and brain retention time than trans isomer [93].

#### 4.1.2. SNS/P nitrido complex

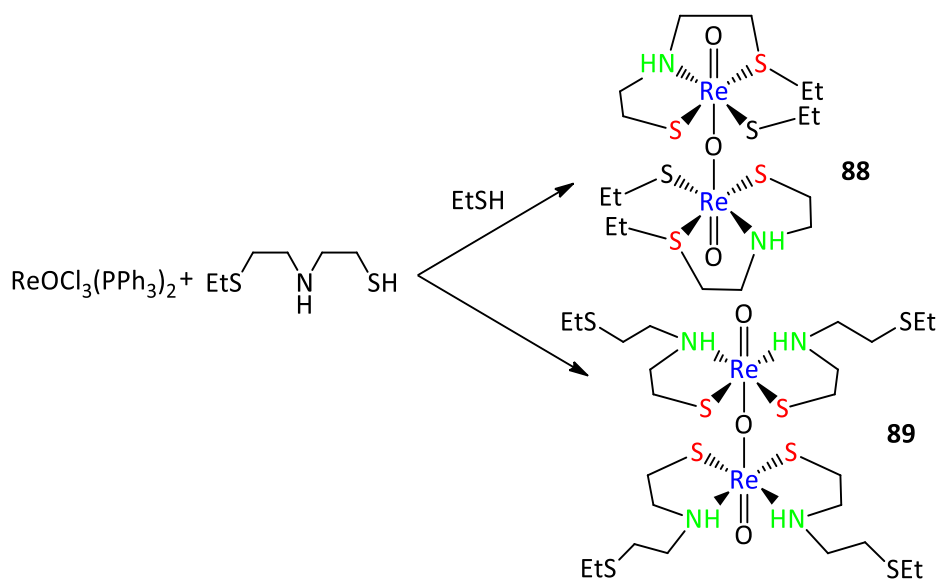
Boschi et al. reported Tc-complex (75, 76) of dianionic tridentate chelating ligand (dimercaptodiethylamine) with metallic fragment  $[MN]^{2+}$  ( $M = Tc, Re$ ) which can exist in two forms namely syn and anti (Chart 25). The increase of sulfur content results in a decrease of

nitrogen content and hence a decrease in lipophilicity has been observed. The combination of the tridentate-donor ligand 2,2'-iminodiethanethiol ( $H_2SNS$ ) and a monodentate-acceptor phosphine provides a simple model for studying the behavior of five-coordinate Tc(V) and Re(V)-nitrido complexes with a mixed coordination environment based on 3 + 1 concept [180].

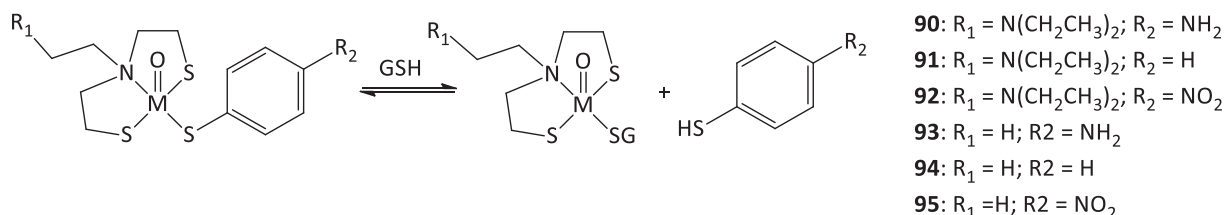
#### 4.1.3. 3 + 2 Systems- SNS/PO

Chiotellis et al. reported the Re(V) complexes of mixed tridentate (aminodithiolate) and bidentate (phosphino phenolate) ligands. It has been further reported that SNS/PO is more lipophilic and hence more efficient in comparison to SNS/N-related systems [182]. The anti isomer of 3 + 1 system is less favorable because it penetrates the blood-brain barrier. The 3 + 2 strategies always result in the formation of syn isomer which is more desirable and stable. The six-coordinate mixed-ligand oxo-Re(V) complexes (77–79) with varying substituents on the central nitrogen atom have been reported (Scheme 18). GSH exchange reaction is observed

in all three complexes (77–79). All of them survived on exposure to a high excess of GSH at physiological pH in contrast to the respective SNS/S (3 + 1 systems), which were rapidly converted to GS-X ( $X = S, PO$ )



**Scheme 21.** Effect of addition of additional reagent for the synthesis of oxorhenium complexes.



**Scheme 22.** The GSH exchange in Tc-/Re-oxo complexes.

hydrophilic species [182]

Recently, Maia et al. reported 3 + 2 mixed ligand complexes of thiosemicarbazone (**80–83**) with varying anion (chloride or bromide) (Scheme 19) [183]. The Tc complex of the thiosemicarbazone ligand has also been synthesized and studied for bioimaging purposes [184].

#### 4.2. Factor affecting the synthesis of bioimaging complexes

##### 4.2.1. Ratio effect

The reactant ratio is particularly significant in the creation of such complexes and may be useful for building the desired complex with a specific activity. The modification of metal precursor, coligand, and ligand ratios results in the production of several new compounds (Scheme 20). The 1:1:1 ratio of metal:HSC<sub>6</sub>H<sub>4</sub>Cl:H<sub>2</sub>L produces neutral syn and anti (**84**, **85**) complexes whereas with 3:0:2 ratio produces binuclear complex **86**. A 1:4:0 ratio of metal:HSC<sub>6</sub>H<sub>4</sub>Cl:H<sub>2</sub>L produces **87** (Scheme 20). Different Tc complexes have also been synthesized by using different ratios and <sup>99m</sup>Tc glucoheptone precursors [181].

##### 4.2.2. Reactant effect

G. Patsis synthesized binuclear complexes instead of pentacoordinate complexes by varying the reactant ratio. The metal salt:SNS:SR ratio 1:1:1 resulted in the formation of complex **88** (Scheme 21). The oxo bridged oxorhenium complex **89** has been produced in the absence of RSH. This indicates that the reagents play an important role in the synthesis of mixed ligand oxorhenium complexes [98].

#### 4.3. In silico study

Preliminary evaluation based on the structure was done using computational SAR analysis for generating drugs with desire activity

**Table 2**

Reactivity data of GSH with varying substituent on nitrogen of SNS and thiols (retention time is in minutes)

Complex	R <sup>1</sup>	R <sup>2</sup>	Tc	Re
<b>90</b>	N(CH <sub>2</sub> CH <sub>3</sub> ) <sub>2</sub>	NH <sub>2</sub>	28.1	27.9
<b>91</b>	N(CH <sub>2</sub> CH <sub>3</sub> ) <sub>2</sub>	H	29.7	29.4
<b>92</b>	N(CH <sub>2</sub> CH <sub>3</sub> ) <sub>2</sub>	NO <sub>2</sub>	30.7	30.4
<b>93</b>	H	NH <sub>2</sub>	26.1	25.9
<b>94</b>	H	H	27.5	27.3
<b>95</b>	H	NO <sub>2</sub>	29	28.7

and minimal side effects. The complexes are being synthesized and subjected to clinical trials only after the SAR analysis give a positive result. Based on the findings of the SAR analysis, the following conclusions can be made;

1. The aromatic ring results in a higher brain uptake and higher brain/blood ratios.
2. Brain retention can be enhanced by introducing bulky substituents at the para position of coligand.
3. Syn isomer has high activity compared to anti isomer for brain uptake and retention.
4. Protonated N has higher activity than unprotonated nitrogen.
5. Electron-withdrawing group (–I group) can enhance the activity.

The substituents attached to the donor atom of and mono-/tri-dentate ligand influence the brain uptake and retention and thus overall bio-distribution [93,103,177,178,185]. These have been further validated by GSH exchange reaction and bio-distribution in the mice model. Gupta et al. showed that the introduction of N-atom has a destabilizing effect and thus the retention time decreases. Retention time increases with

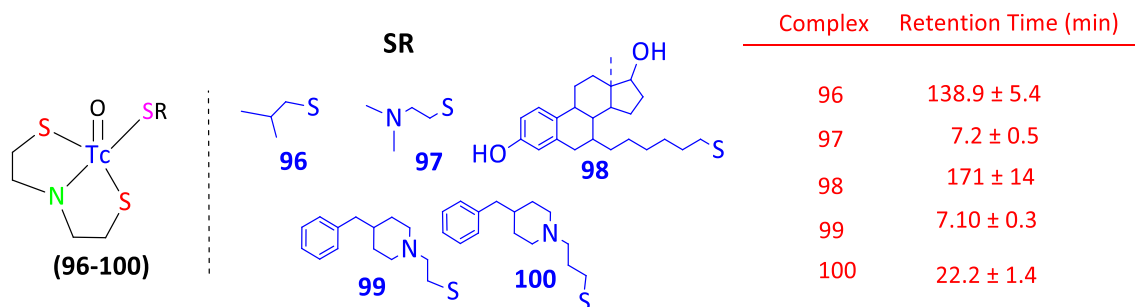


Chart 26. Effect of substituent's on retention time.

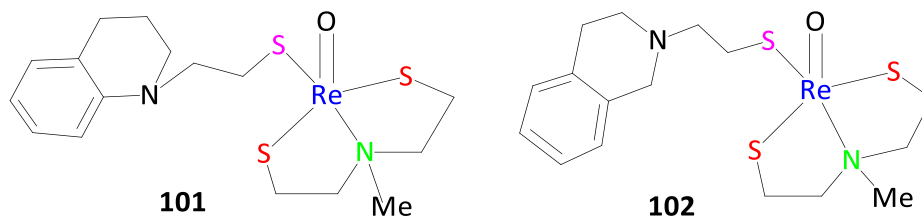


Chart 27. Oxorhenium complexes of SNS and tetrahydroquinoline / tetrahydroisoquinoline.

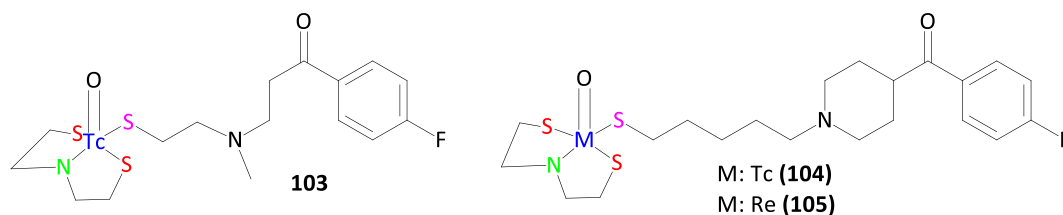


Chart 28. Complexes 103–105 for the imaging of dopamine transporter.

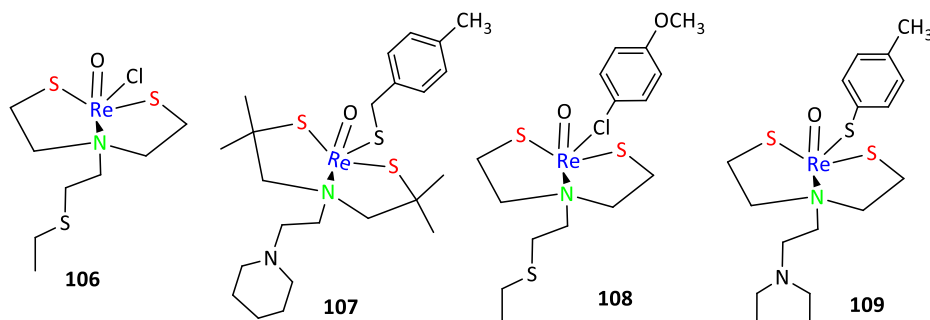


Chart 29. '3 + 1' mixed ligand oxorhenium complexes.

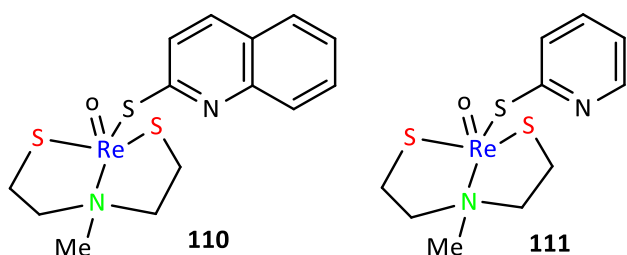
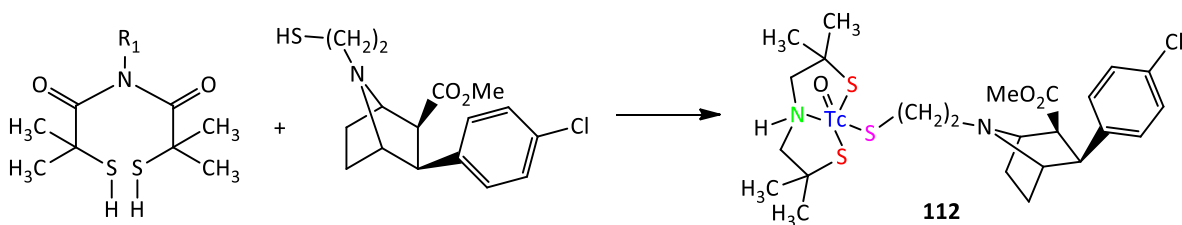


Chart 30. Pyridine and quinoline derivative of SNS complexes.

increasing the carbon chain length between the metal core and the nitrogen atom [103]. Furthermore, the introduction of the -I group on N-atom increases the brain retention time [96,186].

#### 4.4. In vitro study: GSH (Glutathione) conversion and prediction of the stability of complexes

GSH is believed to mediate brain absorption and retention time which is determined by the exchange reaction  $RS^-$  with GSH (Scheme 22). It is an antioxidant that protects against oxidative injury. In 1999, Nock et al. [187] synthesized various Tc and Re complexes (90–95) by substituting electron-donating ( $-NH_2$ ) and electron-withdrawing



Scheme 23. Synthesis of tropane complex as dopamine transporters.

Table 3  
ST/CB ratio for complex 112

S. No.	Organ	2 min	60 min	120 min
1	Cerebellum	0.066 ± 0.017	0.018 ± 0.001	0.011 ± 0.020
2	Saratum	0.054 ± 0.010	0.063 ± 0.001	0.031 ± 0.003
3	Hippocampus	0.046 ± 0.005	0.025 ± 0.000	0.011 ± 0.000
4	Cortex	0.060 ± 0.009	0.026 ± 0.003	0.015 ± 0.003
5	ST/CB ratio	0.82	3.5	2.8

(-NO<sub>2</sub>) groups para to SH and by substituting central 'N' atom of SNS (Scheme 22). The reactivity of complexes with GSH has been found to depend on SNS as well as thiol ligand. The substitution of thiol group follows the order; -NO<sub>2</sub> >> -H > -NH<sub>2</sub>.

GSH and Tc-SNS/S have been studied at the tracer level and showed high brain uptake and retention (Table 2). The replacement of the co-ligand 4-methoxythiophenol by glutathione shows GSH conversion and it can conclude that the brain uptake and retention is GSH mediated process [95].

Gupta et al. observed the effect of different substituents on 'S' on retention time [103]. Five oxotechnetium complexes (96–100) have been synthesized and a comparative study has been carried out. The complexes 96 and 98 showed good retention values (Chart 26).

In 2007, Zablotskaya et al. synthesized oxorhenium complexes of SNS and tetrahydroquinoline (101) / tetrahydroisoquinoline (102) (SNS/S) (Chart 27). Both complexes showed psychotropic activity, hexenal anesthesia, and anticonvulsive activity. Complex 101 has been found more active for hexenal-induced narcosis. However, 102 has been found suitable for carbazole-induced convulsions. The anticancer activity has also been tested against HT-1080 and SHSY5Y cell lines [188].

Johannsen et al. synthesized complexes 103–105 (Chart 28) and used them as a serotonin antagonist and evaluated their activity. Complex 103 has been utilized as a brain imaging agent. Complexes 104 and 105 have been used for the imaging of dopamine transporter. Autoradiographic studies indicate the accumulation of the <sup>99m</sup>Tc in 5-HT(2A)-receptor-rich areas of the brain [102].

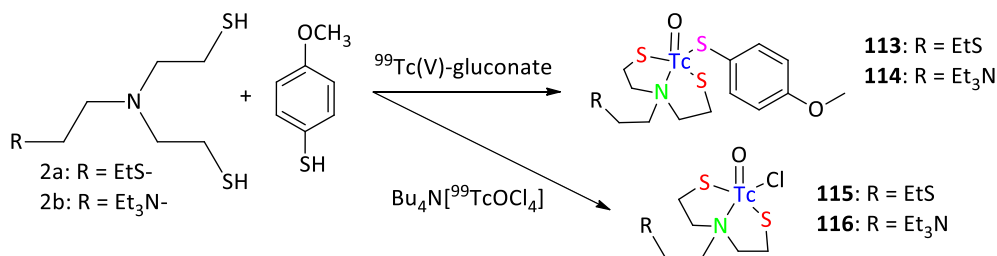
Fietz et al. reported [3-(benzyl)azapentane-1,5-3,3-dithiolato]iodo-oxorhenium (V) complex with 1-β-D-thiogalactose [189]. Palecanou et al. reported four '3 + 1' mixed ligand oxorhenium complexes (106–109) (Chart 29). Complex 108 was prepared at the tracer <sup>186</sup>Re level [94]. Preliminary experiments revealed that the complex <sup>186</sup>Re has

Table 4  
Brain uptake data of complex 113 and 114 with the different time

Complex	Time (min.)				
	1	5	10	30	60
113	2.07	4.53	4.23	1.68	0.60
114	2.49	4.42	4.72	4.16	4.23

Table 5  
Biodistribution data of complex 122 and 125 in mice at 1, 10, and 45 mins after post projection

S. No.	Time (min)	Br/Bi	IC <sub>50</sub>	Complex 125		
				Time	Br/Bi	IC <sub>50</sub>
Complex 122						
1	1	0.81	6	1	0.09	10
2	10	1.70		10	0.31	
3	45	0.97		45	0.30	



Scheme 24. Synthesis of brain imaging agents 113 and 114.

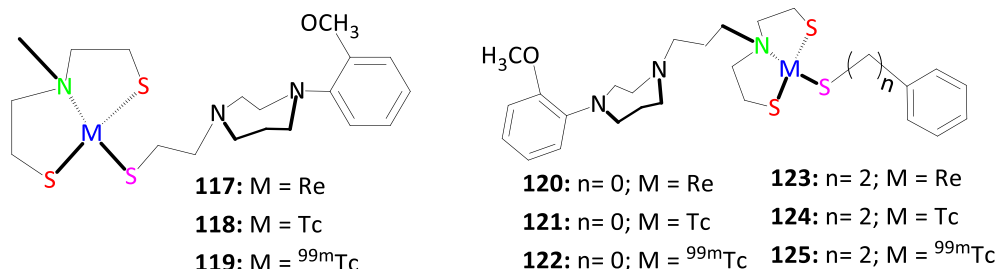
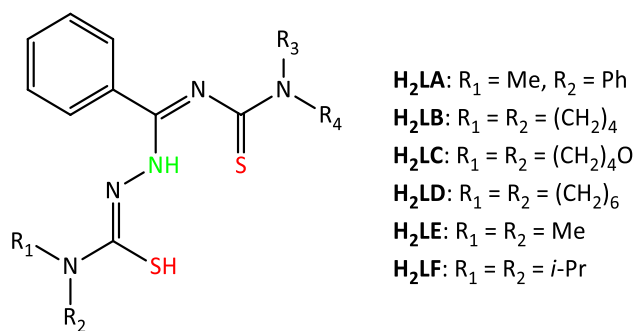


Chart 31. Piperazine derivative as a serotonin antagonist.

Chart 32. Structure of ligands H<sub>2</sub>LA – H<sub>2</sub>LF.

a biodistribution pattern comparable to complex <sup>99m</sup>Tc. It is found that the mixed ligand systems can be used to generate target-specific radiopharmaceuticals (<sup>186/188</sup>Re) for therapeutic applications. Rhenium complexes show a deshielding effect around the metal core as compared to technetium.

In 2012, Segal et al. reported oxorhenium complexes of 3-methylazapentane-1,5-dithiolate and monodentate quinoline / pyridine (**110**, **111**) (Chart 30) and examined their cytotoxic activity towards hepatoma MG-22A [190].

#### 4.5. In-vivo study: Biodistribution of the drug

Mice are the primary models which are used in bio-distribution investigations. Dopamine and serotonin are neurotransmitters that modulate body heat and appetites respectively, with dopamine being associated with pleasant experiences. Their specific level in the body should always be regulated. The imbalance leads to significant mental illnesses including Alzheimer's disease, schizophrenia, anxiety, sadness, and suicide. The complex with different substituents has been used to diagnose psychiatric activity [91,101]. Tropane complex **112** has shown the highest activity as dopamine transporters based on the retention time. The synthesis of this complex is described in Scheme 23. The biodistribution of complex **112** among different body organs

such as the cerebellum, striatum, hippocampus, and cortex was studied. The data showed less brain uptake with adequate clearance

with time with an ST/CB ratio of 3.50 after 60 mins. of injection (Table 3) [101].

Mastrostamatis et al. synthesized four complexes (**113–116**) and the bio-distribution in mice was evaluated. Good initial brain uptake as 3.68 and 3.56% has been observed. The complex containing NEt<sub>3</sub> group at central "N" showed good blood/brain ratio compared to complexes containing SEt group at central "N". Tracer level synthesis was also done (Scheme 24) and complexes **113/114** have been evaluated as a potential brain imaging agent in mice model (Table 4). Labeling has been carried out using <sup>99m</sup>Tc-glucoheptonate as a precursor [91,191].

Paggiannopoulou et al. reported piperazine (**117–125**) derivative (a serotonin antagonist) with trace metals (Chart 31) [192,193]. These complexes showed promising results with good brain/blood retention. The cytotoxic activity has also been examined and a low IC<sub>50</sub> value was observed (Table 5) [192].

Table 6

IC<sub>50</sub> values of ligands Au complexes **126–143** [Au(III)(L)X].

Ligands	IC <sub>50</sub> values			
	H <sub>2</sub> L	[Au(III)(L)Cl]	[Au(III)(L)SCN]	[Au(III)(L)CN]
H <sub>2</sub> LA	0.85	0.68	0.99	
H <sub>2</sub> LB	2.19	0.61		
H <sub>2</sub> LC	0.74	0.63	0.35	0.025
H <sub>2</sub> LD	2.43	0.66		0.045
H <sub>2</sub> LE	0.23	0.66		
H <sub>2</sub> LF	9.04	0.85		

Table 7

IC<sub>50</sub> (μM) values for Re-SNS complex against HCT 116, MCF7, and PC3 cell lines

Complex	IC <sub>50</sub> values for different cancer cell line		
	HCT116	MCF7	PC3
<b>144</b>	25.5 ± 2.5	50.0 ± 8.0	54.0 ± 8.5
<b>145</b>	17.5 ± 3.5	32.0 ± 5.5	23.0 ± 2.5
<b>146</b>	17.0 ± 5.0	24.5 ± 4.5	36.0 ± 10.0
<i>cis</i> -Platin	18.0 ± 2.0	25.0 ± 4.0	16.0 ± 3.0

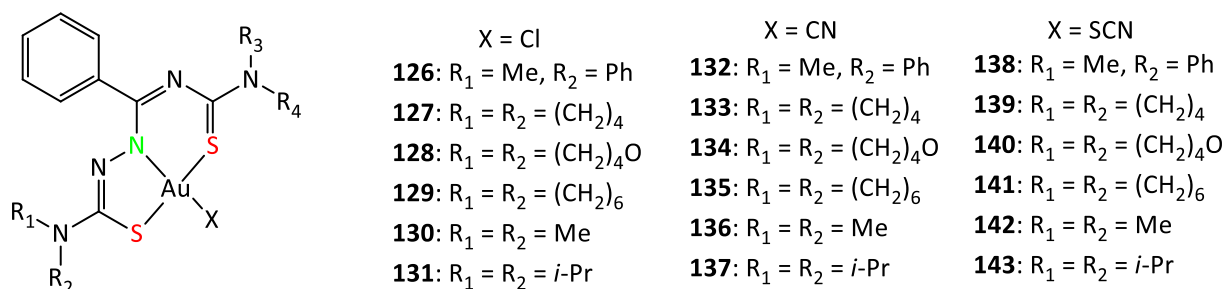


Chart 33. Au-SNS complexes having anticancer and antiparasitic properties.

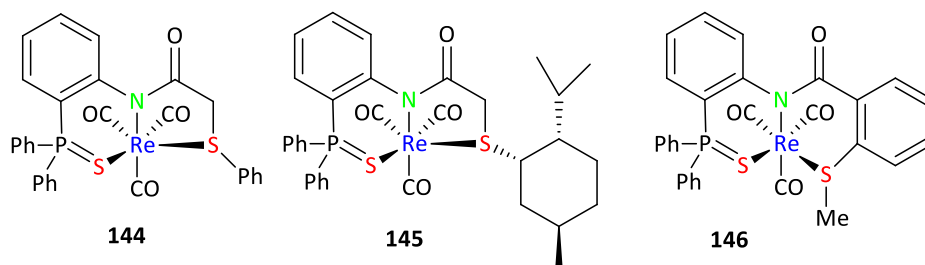


Chart 34. Re-SNS complexes for cancer treatment.

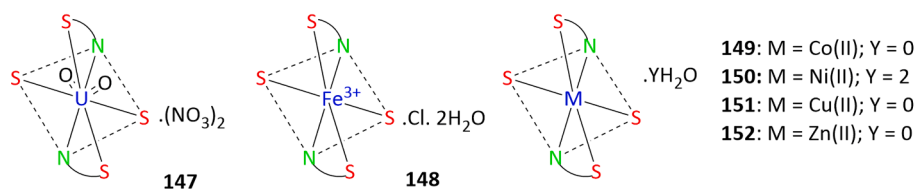


Chart 35. Biological important SNS ligand and complexes.

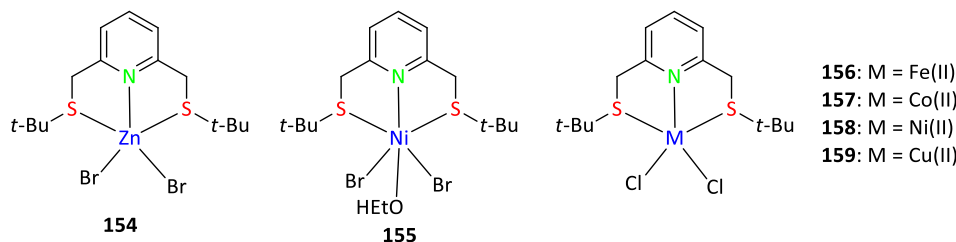


Chart 36. Biological active tbtmp containing complexes.

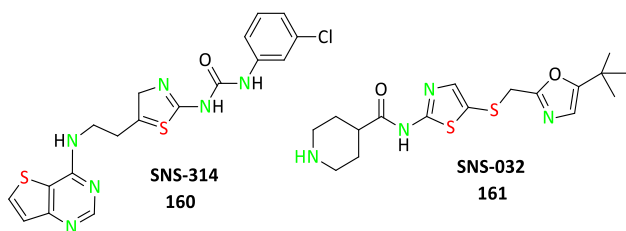


Chart 37. Aurora kinase inhibitor SNS-314 and SNS-032.

## 5. Other biomedical application

### 5.1. Cytotoxicity and antitrypanocidal activity of Au-SNS complexes

Maia et al. synthesized ligands ( $H_2LA-H_2LF$ ) (Chart 32) and their anticancer activity has been examined against MCF-7 cells [194–196]. The Au complexes of these ligands (126–143)  $[Au(III)(L)X]$  (where:  $X = Cl / SCN / CN$ ) (Chart 33) have also been reported and their anticancer activity has been examined against MCF-7 cells. These complexes exhibited cytotoxic as well as antiparasitic activity. These complexes target parasites as well as tumor cells and follow a multi-target mode of mechanism. Antiparasitic activity has been observed with chloro derivatives

126–131 which produce intracellular oxygen species. Furthermore, their activity has been compared with the reference drug benznidazole [194,195]. The  $IC_{50}$  values of ligands and complexes are given in Table 6. The complex containing cyano as coligand 132–137, showed higher anticancer activity as compared to those having chloro/thiocyanate as coligand (126–131 and 138–143) [194,195]. The complex 130, which is a dimethyl derivative of semicarbazone, showed the highest antiparasitic activity for Chagas disease [105].

### 5.2. Cytotoxicity of Re-SNS complex

Three Re(I) tricarbonyl complexes (144–146) of multidentate pincer ligands based on functionalized monothiooxamides have been reported by Kozlov et al. (Chart 34). These complexes have been screened for their cytotoxic activity against HCT116, PC3, and MCF7 cancer cell lines and found to be promising (Chart 4). The results of cytotoxic studies have been compared with the standard drug *cis*-Platin and summarized in Table 7.

The complexes 144 and 146 showed good activity even better than reference drug *cis*-platin as evident from Table 7. The complex 145

showed moderate cytotoxic activity and comparable  $IC_{50}$  values [197].

### 5.3. Antibacterial activity

The SNS Schiff base ligand has been synthesized via condensation of 2-thiophene carboxaldehyde and 2-aminothiophenol. Several metal complexes (147–153) of this ligand (154) have been synthesized (Chart 35) and tested for antibacterial and antifungal activity. Metal complexes were found more effective than the parent Schiff base ligand [198].

A novel tridentate acyclic pincer ligand (tbtmp) and their metal complexes (154–159) with iron, zinc, nickel, cobalt and copper have been reported (Chart 36). The metal complexes showed biological activities but significantly low as compared to standard medicine amphotericin and tetracycline [199].

### 5.4. Kinase inhibitor

The SNS-314 (160) (Chart 37) has been used for cancer treatment as an aurora kinase inhibitor [113]. The SNS-032 (161) has also been tested for aurora kinase-mTORC1/mTORC2 inhibitor [108,110]. SNS-314 mesylate is available in the market as medicine as have  $IC_{50}$  values of 9, 31 and 6 nm for aura A, B and C respectively.

### 5.5. Future perspective

Although SNS ligands are explored to mimic the enzyme along with the biomedical application, however, there is huge scope in this area. A limited number of metals has been complexed with such ligands and thus other metals complexes can be designed which could mimic the metalloenzymes. Metals such as V, Mo etc. can be utilized for this purpose. It has also been observed that the substituents control the activity of the resulting complexes. Thus, new complexes having different substituents in the framework of SNS ligand can be designed which could have different activity than the existing ones. Furthermore, new chemosensors based on SNS donors can be fabricated for the detection of metal ions / anions, molecules and pollutants. The Gd, Eu, and Ir metals have been little explored with SNS ligands. Thus, such metals can be explored for imaging and labeling purposes.

### 5.6. Disadvantages

Although the SNS ligated system has numerous advantages, it is also important to consider their downsides, which have been summarized below;

1. Sulfur-containing chemicals can harm the human body and can cause hair, skin, and other health issues.

2. Radioactive metals technetium and rhenium which are commonly used as bioimaging agents are detrimental to the body. Tc is a weak  $\beta$  emitter and hence proper radiation safety procedures must be followed at all times to avoid contamination and inhalation of such radioactive materials.

3. The synthesis of mixed ligand systems  $3 + 1 / 3 + 2$  is challenging for the designing of neutral oxotechnetium complexes.

4. The synthesis of the model complex is a difficult task that cannot be carried out everywhere.

5. Appropriate regulation must be followed for the storage and use of such reagents.

## 6. Conclusions

This review provides an overview of the role of SNS ligands and their complexes in biological applications. It also discusses the role of SNS donor ligands as enzyme mimics. Furthermore, the significance of SNS ligands as chemosensors and imaging agents has been explored. Many enzymes and proteins such as bsthione, thiolate, semicarbazone, and thioamide have structural relevance to SNS skeletons. To show the enzyme mimic, dinuclear and trinuclear complexes with distinct shapes such as diamond core and butterfly have been reported. Chemosensing is based on the chelating property of the SNS ligand due to their mixed donor atom set. It may be easily examined using various absorption–emission spectroscopy such as UV–Vis, fluorescence and phosphorescence. These methods can also be used for cation / anion and molecule detection. For imaging purposes, the designing of complexes is very important as increasing lipophilicity is easily absorbed by body organs and plays an important role in diagnostic and therapeutic applications. Sulfur inclusion in the ligands framework has been shown to considerably impact lipophilicity, allowing for simple absorption of such systems by body organs. Although such systems have been reported, however, there are huge scopes to develop new S donor ligands, their metal complexes and explore their ability to mimic enzymes and in medicine.

## Declaration of Competing Interest

The authors declare that they have no known competing financial interests or personal relationships that could have appeared to influence the work reported in this paper.

## Acknowledgments

P.O. acknowledges DST for INSPIRE Fellowship [DST/INSPIRE Fellowship/2017/IF170491]. GKR acknowledges the support provided under the DST-FIST Grant No. SR/FST/PSI/2018/48 of Government of India. A.K. acknowledges Science and Engineering Research Board (SERB), New Delhi, India for fellowship through the project [ECR/2016/001549].

## References

- [1] H.G. Sogukomerogullari, Ş.P. Yalçın, Ü. Ceylan, E. Aytar, M. Aygün, D. S. Richeson, M. Sönmez, *J. Chem. Sci.* 131 (2019) 32–44.
- [2] E. Ahmadi, Z. Mohamadnia, *Catal. Lett.* 141 (2011) 1191–1198.
- [3] C.N. Temple, S. Gambarotta, I. Korobkov, R. Duchateau, *Organometallics* 26 (2007) 4598–4603.
- [4] J. Schörgenhumer, A. Zimmermann, M. Waser, *Org. Process Res. Dev.* 22 (2018) 862–870.
- [5] S.Q. Bai, T.S.A. Hor, *Chem. Commun.* 672 (2008) 3172–3174.
- [6] H.G. Sogukomerogullari, E. Aytar, M. Ulusoy, S. Demir, N. Dege, D.S. Richeson, M. Sönmez, *Inorganica Chim. Acta* 471 (2018) 290–296.
- [7] M.R. Elsby, R.T. Baker, *Chem. Commun.* 55 (2019) 13574–13577.
- [8] S.P. Midya, V.G. Landge, M.K. Sahoo, J. Rana, E. Balaraman, *Chem. Commun.* 54 (2017) 90–93.
- [9] L. Soobramoney, M.D. Bala, H.B. Friedrich, *Inorganica Chim. Acta* 479 (2018) 97–105.
- [10] L. Soobramoney, M.D. Bala, H.B. Friedrich, *Inorganica Chim. Acta* 526 (2021) 102508–102510.
- [11] Z.J. Mast, T.H.T. Myren, C.G. Huntzinger, T.A. Stinson, R.M. Kharbouch, E. M. Almanza, S.E. Zymont, J.R. Miecznikowski, O.R. Luca, *Inorg. Chem. Front.* 7 (2020) 1012–1015.
- [12] F. Saghatchi, E. Ahmadi, Z. Mohamadnia, *Chem. Pap.* 68 (2014) 1555–1560.
- [13] H. Gamze, E. Aytar, M. Ulusoy, S. Demir, N. Dege, *Inorg. Chim. Acta* 471 (2018) 290–296.
- [14] J. Reglinski, M. Spicer, *Curr. Bioact. Compd.* 5 (2009) 264–276.
- [15] M. Fontecave, G.L. Pierre, *Coord. Chem. Rev.* 170 (1998) 125–140.
- [16] S.W. Ragsdale, *Chem. Rev.* 106 (2006) 3317–3337.
- [17] M. Pellei, C. Santini, *Biomimetic Applications of Metal Systems Supported by Scorpionates*, 2011.
- [18] I. Nath, J. Chakraborty, F. Verpoort, *Chem. Soc. Rev.* 45 (2016) 4127–4170.
- [19] K.D. Karlin, *Science* 261 (1993) 701–708.
- [20] C.A. Dodds, M. Garner, J. Reglinski, M.D. Spicer, *Inorg. Chem.* 45 (2006) 2733–2741.
- [21] G. Nuss, G. Saischek, B.N. Harum, M. Volpe, F. Belaj, N.C. Mösche-Zanetti, *Inorg. Chem.* 50 (2011) 12632–12640.
- [22] A. Majumdar, *Dalton Trans.* 43 (2014) 12135–12145.
- [23] D. Huang, L. Deng, J. Sun, R.H. Holm, *Inorg. Chem.* 48 (2009) 6159–6166.
- [24] M.A. Halcrow, G. Christou, *Chem. Rev.* 94 (1994) 2421–2481.
- [25] D. Sellmann, D. Häußinger, F.W. Heinemann, *Eur. J. Inorg. Chem.* 1999 (1999) 1715–1725.
- [26] J.L. Boer, S.B. Mulrooney, R.P. Hausinger, *Arch. Biochem. Biophys.* 544 (2013) 142–152.
- [27] A. Hemschemeier, T. Happe, *Nat. Rev. Chem.* 2 (2018) 231–243.
- [28] J. Rittle, J.C. Peters, *Proc. Natl. Acad. Sci. U. S. A.* 110 (2013) 15898–15903.
- [29] T.C. Harrop, P.K. Mascharak, *Acc. Chem. Res.* 37 (2004) 253–260.
- [30] Y.N. Chirgadze, E.A. Boshkova, R.V. Polozov, V.S. Sivozhelezov, A. V. Dzyabchenko, M.B. Kuzminsky, V.A. Stepanenko, V.V. Ivanov, *J. Biomol. Struct. Dyn.* 36 (2018) 3902–3915.
- [31] I. Labadi, M. Benko, K. Marko, *React. Kinet. Catal. Lett.* 96 (2009) 327–333.
- [32] A. Shaikh, S. Reza, M. Rahman, P.K. Bakshi, *Dhaka Univ. J. Sci.* 60 (2012) 97–101.
- [33] A.J.T. Smith, R. Muller, M.D. Toscano, P. Kast, H.W. Hellinga, D. Hilvert, K. N. Houk, *J. Am. Chem. Soc.* 130 (2008) 15361–15373.
- [34] I. Castillo, *Transition Metal Complexes with Anionic Sulfur-Based Pincer Ligands*, Elsevier Inc., 2018.
- [35] A. Panja, D.M. Eichhorn, *Inorganica Chim. Acta* 391 (2012) 88–92.
- [36] Y.M. Albkuri, J.S. Ovens, J. Martin, R.T. Baker, *Inorg. Chem.* 60 (2021) 10934–10942.
- [37] S. Thanneeru, J.K. Nganga, A.S. Amin, B. Liu, L. Jin, A.M. Angeles-Boza, J. He, *ChemCatChem* 9 (2017) 1157–1162.
- [38] A. Mondragón, M. Flores-Alamo, P.R. Martínez-Alanis, G. Aullón, V.M. Ugalde-Saldívar, I. Castillo, *Inorg. Chem.* 54 (2015) 619–627.
- [39] E.R. Marín, A. Mondragón, R. Paulina, M. Alanis, G. Aullón, M.F. Alamo, I. Castillo, *Dalton Trans.* 47 (2018) 10932–10940.
- [40] A. Mondragón, P.R. Martínez-Alanis, G. Aullón, S. Hernández-Ortega, E. Robles-Marín, M. Flores-Alamo, V.M. Ugalde-Saldívar, I. Castillo, *Dalt. Trans.* 45 (2016) 9996–10006.
- [41] R.A. Begum, D. Powell, K. Bowman-James, *Inorg. Chem.* 45 (2006) 964–966.
- [42] U.K. Das, S.L. Daifuku, T.E. Iannuzzi, S.I. Gorelsky, I. Korobkov, B. Gabidullin, M. L. Neidig, R. Tom Baker, *Inorg. Chem.* 56 (2017) 13766–13776.
- [43] J.R. Sunderland, X. Tao, E.E. Butrick, L.C. Keilich, C.E. Villa, J.R. Miecznikowski, S.S. Jain, *Polyhedron* 114 (2016) 145–151.
- [44] S.B. Harkins, J.C. Peters, *J. Am. Chem. Soc.* 126 (2004) 2885–2893.
- [45] B. Desguin, P. Goffin, E. Viaene, M. Kleerebezem, V. Martin-Diaconescu, M. J. Maroney, J.-P. Declercq, P. Soumillion, P. Hols, *Nat. Commun.* 5 (2014) 3615–3626.
- [46] K. Kaldunská, A. Kozakiewicz, M. Wujak, A. Wojtczak, *Materials* 14 (2021) 3250–3273.
- [47] S. Brander, I. Horvath, J. Ipsen, A. Peculyte, L. Olsson, C. Hernández-Rollán, M. H.H. Nørholm, S. Mossin, L. Lo Leggio, C. Probst, D.J. Thiele, K.S. Johansen, *Sci. Rep.* 10 (2020) 16369–16379.
- [48] Y. Jiang, L.R. Widger, G.D. Kasper, M.A. Siegler, D.P. Goldberg, *J. Am. Chem. Soc.* 132 (2010) 12214–12215.
- [49] D.V. Aleksanyan, V.A. Kozlov, Y.V. Nelyubina, K.A. Lyssenko, L.N. Puntus, E. I. Gutsul, N.E. Shepel, A.A. Vasil'Ev, P.V. Petrovskii, I.L. Odinets, *Dalton Trans.* 40 (2011) 1535–1546.
- [50] H. Kirpik, M. Kose, J.N. Balli, *Appl. Organomet. Chem.* 34 (2020) 1–11.
- [51] V. Sathish, A. Ramdass, M. Velayudham, K.L. Lu, P. Thanasekaran, S. Rajagopal, *Dalton Trans.* 41 (2017) 11497–11506.
- [52] H. Zhu, J. Fan, B. Wang, X. Peng, *Chem. Soc. Rev.* 2014.
- [53] X.Y. Wang, A.D. Guerso, R.H. Schmehl, *J. Photochem. Photobiol. C: Photochem. Rev.* 5 (2004) 55–57.
- [54] X. Liu, J. Hamon, *Coord. Chem. Rev.* 389 (2019) 94–118.
- [55] H.X. Zhang, M. Kato, Y. Sasaki, T. Ohba, H. Ito, A. Kobayashi, H.C. Chang, K. Uosaki, *Dalton Trans.* 41 (2012) 11497–11506.
- [56] V. Brune, C. Hegemann, S. Mathur, *Inorg. Chem.* 58 (2019) 9922–9934.
- [57] L. Duan, Y. Xu, X. Qian, *Chem. Commun.* (2008) 6339–6341.
- [58] B. Kaur, N. Kaur, S. Kumar, *Coord. Chem. Rev.* 358 (2018) 13–69.
- [59] A. Ramdass, V. Sathish, E. Babu, M. Velayudham, P. Thanasekaran, S. Rajagopal, *Coord. Chem. Rev.* 343 (2017) 278–307.

- [60] K. Okamoto, T. Yamamoto, M. Akita, A. Wada, T. Kanbara, *Organometallics* 28 (2009) 3307–3310.
- [61] S. Ghosh, A.S. Alghunaim, M.H. Al-Mashhadani, M.P. Krompiec, M. Hallett, I. F. Perepichka, *J. Mater. Chem. C* 6 (2018) 3762–3773.
- [62] M. Sarkar, S. Banthia, A. Samanta, *Tetrahedron Lett.* 47 (2006) 7575–7578.
- [63] A. Degirmenci, D. Iskenderkaptanoglu, F. Algi, *Tetrahedron Lett.* 56 (2014) 602–607.
- [64] T.F. Otero, S. Villanueva, E. Brillas, J. Carrasco, *Synth. Met.* 102 (1999) 1402–1403.
- [65] T.F. Otero, J. Carrasco, A. Figueras, E. Brillas, *J. Electroanal. Chem.* 370 (1994) 231–239.
- [66] T.E. Wood, A. Thompson, *Chem. Rev.* 107 (2007) 1831–1861.
- [67] F. Algi, A. Cihaner, *Polymer* 53 (2012) 3469–3475.
- [68] N. Guven, P. Camurlu, *Polymer* 73 (2015) 122–130.
- [69] J.P. Ferraris, M.D. Newton, *Polymer* 33 (1992) 391–397.
- [70] J.P. Ferraris, R.G. Andrus, D.C. Hrnrcir, *J. Chem. Soc. Chem. Commun.* (1989) 1318–1320.
- [71] E. Yildiz, P. Camurlu, C. Tanyeli, I. Akhmedov, L. Toppare, *J. Electroanal. Chem.* 612 (2008) 247–256.
- [72] F. Ekiz, F. Ouzkaya, M. Akin, S. Timur, C. Tanyeli, L. Toppare, *J. Mater. Chem.* 21 (2011) 12337–12343.
- [73] A. Yavuz, B. Bezgin, L. Aras, A.M. Önal, *J. Electroanal. Chem.* 639 (2010) 116–122.
- [74] Arzu Yavuz, Buket Bezgin C, arbas, Leyla Aras, *J. Appl. Polym. Sci.* 116 (2010) 1293–1299.
- [75] A. Cihaner, F. Algi, *Electrochim. Acta* 54 (2009) 1702–1709.
- [76] A. Cihaner, F. Algi, *J. Electroanal. Chem.* 614 (2008) 101–106.
- [77] F. Algi, A. Cihaner, *Tetrahedron Lett.* 49 (2008) 3530–3533.
- [78] A. Cihaner, F. Algi, *Turkish J. Chem.* 33 (2009) 759–767.
- [79] A. Cihaner, F. Algi, *Electrochim. Acta* 53 (2008) 2574–2578.
- [80] D. Asil, A. Cihaner, F. Algi, A.M. Önal, *J. Electroanal. Chem.* 22 (2010) 2254–2260.
- [81] A. Yavuz, B. Bezgin, A.M. Onal, *J. Appl. Polym. Sci.* 114 (2009) 2685–2690.
- [82] S. Eken, B.B. Carbas, A. Akdag, A.M. Önal, *J. Electrochem. Soc.* 161 (2014) G115–G121.
- [83] A. Arslan, Ö. Türkarlan, C. Tanyeli, I.M. Akhmedov, L. Toppare, *Mater. Chem. Phys.* 104 (2007) 410–416.
- [84] E. Sahin, E. Sahmetlioglu, I.M. Akhmedov, C. Tanyeli, L. Toppare, *Org. Electron.* 7 (2006) 351–362.
- [85] E. Deutsch, K. Libson, J.L. Vanderheyden, A.R. Ketring, H.R. Maxon, *Int. J. Rad. Appl. Instrum. B* 13 (1986) 465–477.
- [86] M. Pelecanou, K. Chryssou, C.I. Stassinopoulou, *J. Inorg. Biochem.* 79 (2000) 347–351.
- [87] R. Southworth, T.M.de Rosales, L.K. Meszaros, M.T. Ma, G.E.D. Mullen, G. Fruhwirth, J.D. Young, C. Imberti, J. B.-Torres, E. Andreozzi, P.J. Blower, *Adv. Inorg. Chem.* 68 (2016) 1–41.
- [88] T.N. Rao, A.R. Fritzberg, D. Adhikesavalu, A. Camerman, A.R. Fritzberg, *J. Am. Chem. Soc.* 112 (1990) 5798–5804.
- [89] A.A. Holder, *Annu. Reports Prog. Chem. - Sect. A* 107 (2011) 359–378.
- [90] Z.P. Zhuang, K. Plössl, M.P. Kung, M. Mu, H.F. Kung, *Nucl. Med. Biol.* 26 (1999) 217–224.
- [91] S.G. Mastrostamatis, M.S. Papadopoulos, I.C. Pirmettis, E. Paschali, A. D. Varvarigou, C.I. Stassinopoulou, C.P. Raptopoulou, A. Terzis, E. Chiotellis, *J. Med. Chem.* 37 (1994) 3212–3218.
- [92] M. Papadopoulos, C. Tsoukalas, I. Pirmettis, B. Nock, T. Maina, Z. Abedin, C. P. Raptopoulou, A. Terzis, E. Chiotellis, *Inorganica Chim. Acta* 285 (1999) 97–106.
- [93] M.S. Papadopoulos, I.C. Pirmettis, M. Pelecanou, C.P. Raptopoulou, A. Terzis, C. I. Stassinopoulou, E. Chiotellis, *Inorg. Chem.* 35 (1996) 7377–7383.
- [94] M. Pelecanou, I.C. Pirmettis, M.S. Papadopoulos, C.P. Raptopoulou, A. Terzis, E. Chiotellis, C.I. Stassinopoulou, *Inorganica Chim. Acta* 287 (1999) 142–151.
- [95] M. Pelecanou, C. Pirmettis, A. Nock, M. Papadopoulos, E. Chiotellis, I. Stassinopoulou, *Inorganica Chim. Acta* 281 (1998) 148–152.
- [96] C.H. Tsoukalas, I. Pirmettis, G. Patsis, A. Papadopoulos, C.P. Raptopoulou, A. Terzis, M. Papadopoulos, E. Chiotellis, *Nucl. Nucl. Med. Biol.* 28 (2001) 975–982.
- [97] I.C. Pirmettis, M.S. Papadopoulos, S.G. Mastrostamatis, C.P. Raptopoulou, A. Terzis, E. Chiotellis, *Inorg. Chem.* 35 (1996) 1685–1691.
- [98] G. Patsis, I. Pirmettis, C. Tsoukalas, M. Pelecanou, C.P. Raptopoulou, A. Terzis, M. Papadopoulos, E. Chiotellis, *Inorg. Chim. Acta* 342 (2003) 272–278.
- [99] I.C. Pirmettis, M.S. Papadopoulos, E. Chiotellis, *J. Med. Chem.* 40 (1997) 2539–2546.
- [100] P. Martini, M. Pasquali, A. Boschi, L. Uccelli, M. Giganti, A. Duatti, *Molecules* 23 (2018) 1–12.
- [101] S. Meegalla, K. Plössl, M.P. Kung, S. Chumpradit, D.A. Stevenson, D. Frederick, H. F. Kung, *Bioconjug. Chem.* 7 (1996) 421–429.
- [102] H.J. Pietzsch, M. Scheunemann, M. Kretzschmar, S. Elz, H.H. Pertz, S. Seifert, P. Brust, H. Spies, R. Syhre, B. Johannsen, *Nucl. Med. Biol.* 26 (1999) 865–875.
- [103] B.A. Gupta, S. Seifert, R. Syhre, M. Scheunemann, P. Brust, *Radiochim. Acta* 89 (2001) 43–49.
- [104] H.F. Kung, S. Meegalla, M.P. Kung, K. Plössl, *Transit. Met. Chem.* 23 (1998) 531–536.
- [105] C.D. Lopes, B. Possato, A.P.S. Gaspari, R.J. Oliveira, U. Abram, J.P.A. Almeida, F. D.R. Rocho, A. Leitão, C.A. Montanari, P.I.S. Maia, J.S. Da Silva, S. De Albuquerque Albuquerque, Z.A. Carneiro, *ACS Infect. Dis.* 5 (2019) 1698–1707.
- [106] A. Conroy, D.E. Stockett, D. Walker, M.R. Arkin, U. Hoch, J.A. Fox, R.E. Hawtin, *Cancer Chemother. Pharmacol.* 64 (2009) 723–732.
- [107] E.I. Heath, K. Bible, R.E. Martell, D.C. Adelman, P.M. LoRusso, *Invest New Drug* 26 (2008) 59–65.
- [108] R. Chen, W.G. Wierda, S. Chubb, R.E. Hawtin, J.A. Fox, M.J. Keating, V. Gandhi, W. Plunkett, *Blood* 113 (2009) 4637–4645.
- [109] E. Walsby, M. Lazenby, C. Pepper, A.K. Burnett, *Leukemia* 25 (2011) 411–419.
- [110] N. Löschmann, M. Michaelis, F. Rothweiler, R. Zehner, J. Cinatl, Y. Voges, M. Sharifi, K. Riecken, J. Meyer, A. von Deimling, I. Fichtner, T. Ghafourian, F. Westermann, J. Cinatl, *Transl. Oncol.* 6 (2013) 685–696.
- [111] H. Meng, Y. Jin, H. Liu, L. You, C. Yang, X. Yang, W. Qian, *J. Hematol. Oncol.* 6 (2013) 1–14.
- [112] C.M. Olson, B. Jiang, M.A. Erb, Y. Liang, Z.M. Doctor, Z. Zhang, T. Zhang, N. Kwiatkowski, M. Boukhali, J.L. Green, W. Haas, T. Nomanbhoy, E.S. Fischer, R. A. Young, J.E. Bradner, G.E. Winter, N.S. Gray, *Nat. Chem. Biol.* 14 (2018) 163–170.
- [113] B. Zhang, Y. Li, H. Zhang, C. Ai, *Int. J. Mol. Sci.* 11 (2010) 4326–4347.
- [114] J.P. Arbitrario, B.J. Belmont, M.J. Evanchik, W.M. Flanagan, R.V. Fucini, S. K. Hansen, S.O. Harris, A. Hashash, U. Hoch, J.N. Hogan, A.R. Howlett, J. W. Jacobs, J.W. Lam, S.C. Ritchie, M.J. Romanowski, J.A. Silverman, D. E. Stockett, J.N. Teague, K.M. Zimmerman, P. Taverna, *Cancer Chemother. Pharmacol.* 65 (2010) 707–717.
- [115] E.C. VanderPorten, P. Taverna, J.N. Hogan, M.D. Ballinger, W.M. Flanagan, R. V. Fucini, *Mol. Cancer Ther.* 8 (2009) 930–939.
- [116] J.R. Miecznikowski, W. Lo, M.A. Lynn, S. Jain, L.C. Keilich, N.F. Kloczko, B. E. O’Loughlin, A.P. Dimarzio, K.M. Foley, G.P. Lisi, D.J. Kwiecien, E.E. Butrick, E. Powers, R. Al-Abbese, *Inorganica Chim. Acta* 387 (2012) 25–36.
- [117] M.A. Lynn, J.R. Miecznikowski, J.P. Jasinski, M. Kaur, B.Q. Mercado, E. Reinheimer, E.M. Almanza, R.M. Kharbouch, M.R. Smith, S.E. Zygmont, N. F. Flaherty, A.C. Smith, *Inorganica Chim. Acta* 485 (2019) 118996–119007.
- [118] J.R. Miecznikowski, J.P. Jasinski, K.A. Archer, C.E. Villa, E.G. Lemons, R. M. Kharbouch, S.E. Zygmont, K.R. Landy, *J. Vis. Exp.* 157 (2020) 1–8.
- [119] J.R. Miecznikowski, M.A. Lynn, J.P. Jasinski, W. Lo, D.W. Bak, M. Pati, E. E. Butrick, A.E.R. Drozdowski, K.A. Archer, C.E. Villa, E.G. Lemons, E. Powers, M. Siu, C.D. Gomes, N.A. Bernier, *Polyhedron* 80 (2014) 157–165.
- [120] N. Mahanta, D.M. Szantai-Kis, E.J. Petersson, D.A. Mitchell, A.C.S. Chem. Biol. 14 (2019) 142–163.
- [121] A.K. Jones, B.R. Lichtenstein, A. Dutta, G. Gordon, P.L. Dutton, *J. Am. Chem. Soc.* 129 (2007) 14844–14845.
- [122] C.M. Lee, C.H. Hsieh, A. Dutta, G.H. Lee, W.F. Liaw, *J. Am. Chem. Soc.* 125 (2003) 11492–11493.
- [123] X. Wang, S. Peter, R. Ullrich, M. Hofrichter, J.T. Groves, *Angew. Chemie - Int. Ed.* 52 (2013) 9238–9241.
- [124] U.K. Das, S.L. Daifuku, S.I. Gorelsky, I. Korobkov, M.L. Neidig, J.J. Le Roy, M. Murugesu, R.T. Baker, *Inorg. Chem.* 55 (2016) 987–997.
- [125] A. Bhandari, S. Mishra, R.C. Maji, A. Kumar, M.M. Olmstead, A.K. Patra, *Angew. Chemie - Int. Ed.* 59 (2020) 9177–9185.
- [126] B. Desguin, B. Desguin, M.F.O. Riant, J. Hu, X.R.P. Hausinger, P. Hols, P. Soumillion, *J. Biol. Chem.* 293 (2018) 12303–12317.
- [127] A. Mondragón-Díaz, E. Robles-Marín, B.A. Murueta-Cruz, J.C. Aquite, P. R. Martínez-Alanis, M. Flores-Alamo, G. Aullón, L.N. Benítez, I. Castillo, *Chem. - An Asian J.* 14 (2019) 3301–3312.
- [128] A. Abdollahi, H. Roghani-Mamaqani, B. Razavi, M. Salami-Kalajahi, *ACS Nano* 14 (2020) 14417–14492.
- [129] A. Abdollahi, H. Roghani-Mamaqani, B. Razavi, *Prog. Polym. Sci.* 98 (2019), 101149.
- [130] N. Guven, H. Sultanova, B. Ozer, B. Yuçel, P. Camurlu, *Electrochim. Acta* 329 (2019) 135134–135183.
- [131] J.W. Thackeray, H.S. White, M.S. Wrighton, *J. Phys. Chem.* 89 (1985) 5133–5140.
- [132] N. Guven, P. Camurlu, B. Yuçel, *Polym. Int.* 64 (2015) 758–765.
- [133] R. Brooke, J. Edberg, D. Iandolo, M. Berggren, X. Crispin, I. Engquist, *J. Mater. Chem. C* 6 (2018) 4663–4670.
- [134] S.Ö. Kart, A. Ebru Tanboğa, H.C. Soyleyici, M. Ak, H.H. Kart, *Spectrochim. Acta - Part A Mol. Biomol. Spectrosc.* 137 (2015) 1174–1183.
- [135] D.W. Shaffer, G. Szigethy, J.W. Ziller, A.F. Heyduk, *Inorg. Chem.* 52 (2013) 2110–2118.
- [136] K.E. Rosenkoetter, J.W. Ziller, A.F. Heyduk, *Dalt. Trans.* 46 (2017) 5503–5507.
- [137] K.E. Rosenkoetter, J.W. Ziller, A.F. Heyduk, *Inorg. Chem.* 55 (2016) 6794–6798.
- [138] J.M. Barlow, J.W. Ziller, J.Y. Yang, *ACS Catal.* 11 (2021) 8155–8164.
- [139] B.J. Ye, B.G. Kim, M.J. Jeon, S.Y. Kim, H.C. Kim, T.W. Jang, H.J. Chae, W.J. Choi, M.N. Ha, Y.S. Hong, *Ann. Occup. Environ. Med.* 28 (2016) 1–8.
- [140] K.M. Rice, E.M.W. Jr, M. Wu, C. Gillette, E.R. Blough, *J. Prev. Med. Public Health* 47 (2014) 74–83.
- [141] B.D. Barst, M. Rosabal, P.E. Drevnick, P.G.C. Campbell, N. Basu, *Environ. Pollut.* 242 (2018) 63–72.
- [142] W. Lai, S.M. Berry, D.C. Bebout, R.J. Butcher, *Inorg. Chem.* 45 (2006) 571–581.
- [143] J.G. Egan, A.J. Hynes, H.M. Fruehwald, I.I. Ebralidze, S.D. King, R. Alipour Moghadam Esfahani, F.Y. Naumkin, E.B. Easton, O. V. Zenkina, *J. Mater. Chem. C* 7 (2019) 10187–10195.
- [144] R. Kumar, R. Misra, T.K. Chandrashekar, A. Nag, D. Goswami, E. Suresh, C. H. Suresh, *European J. Org. Chem.* (2007) 4552–4562.
- [145] W.Y. Gao, L. Wojtas, S. Ma, *Chem. Commun.* 50 (2014) 5316–5318.
- [146] J. Sankar, S. Mori, S. Saito, H. Rath, M. Suzuki, Y. Inokuma, H. Shinokubo, S. K. Kil, S.Y. Zin, J.Y. Shin, M.L. Jong, Y. Matsuzaki, O. Matsushita, A. Muranaka, N. Kobayashi, D. Kim, A. Osuka, *J. Am. Chem. Soc.* 130 (2008) 13568–13579.

- [147] A. Srinivasan, V.R.M. Reddy, S. Jeyaprakash Narayanan, B. Sridevi, S.K. Pushpan, M. Ravikumar, T.K. Chandrashekar, *Angew. Chem. - Int. Ed.* 36 (1997) 2598–2601.
- [148] Z. Zhou, Z. Shen, *J. Mater. Chem. C* 3 (2015) 3239–3251.
- [149] C.S. Veliizquez, G.A. Fox, W.E. Broderick, K.A. Andemen, O.P. Anderson, A.G. M. Barrett, B.M. Hoffman, *J. Am. Chem. Soc.* 114 (1992) 7416–7424.
- [150] J.L. Sessler, E. Tomat, *Acc. Chem. Res.* 40 (2007) 371–379.
- [151] D. Wu, A.B. Descalzo, F. Weik, F. Emmerling, Z. Shen, X.Z. You, K. Rurack, *Angew. Chemie - Int. Ed.* 47 (2008) 193–197.
- [152] P.O. Ganrot, *Environ. Health Perspect.* 65 (1986) 363–441.
- [153] Y. Lu, S. Huang, Y. Liu, S. He, L. Zhao, X. Zeng, *Org. Lett.* 13 (2011) 5274–5277.
- [154] A.L. Wani, A. Ara, J.A. Usmani, *Interdiscip. Toxicol.* 8 (2015) 55–64.
- [155] M. Markowitz, *Curr. Probl. Pediatr.* 30 (2000) 62–70.
- [156] R. Ayranci, M. Ak, *New J. Chem.* 40 (2016) 8053–8059.
- [157] R. Ayranci, M. Ak, *J. Electrochem. Soc.* 166 (2019) B291–B296.
- [158] M. Pamuk Algı, Z. Öztas, F. Algı, *Chem. Commun.* 48 (2012) 10219–10221.
- [159] Z. Öztas, M. Pamuk, F. Algı, *Tetrahedron* 69 (2013) 2048–2051.
- [160] B. Liu, Y. Bao, F. Du, H. Wang, J. Tian, R. Bai, *Chem. Commun.* 47 (2011) 1731–1733.
- [161] T. Soganci, H.C. Soyleyici, M. Ak, *J. Electrochem. Soc.* 165 (2018) H941–H953.
- [162] M. Bilmez, A. Degirmenci, M.P. Algı, F. Algı, *New J. Chem.* 42 (2018) 450–457.
- [163] S. Soylemez, T. Yilmaz, E. Buber, Y.A. Udum, S. Özçubukçu, L. Toppare, *J. Mater. Chem. B* 5 (2017) 7384–7392.
- [164] Y. Cui, B. Li, H. He, W. Zhou, B. Chen, G. Qian, *Acc. Chem. Res.* 49 (2016) 483–493.
- [165] C.-X. Zhang, S.-L. Mei, X.-H. Chen, E.-T. Liu, C.-J. Yao, *J. Mater. Chem. C* 9 (2021) 17182–17200.
- [166] S. Varis, M. Ak, C. Tanyeli, I.M. Akhmedov, L. Toppare, *Eur. Polym. J.* 42 (2006) 2352–2360.
- [167] W. Xu, K. Fu, C. Ma, P.W. Bohn, *Analyst* 141 (2016) 6018–6024.
- [168] N. Kobayashi, S. Miura, M. Nishimura, H. Urano, *Sol. Energy Mater. Sol. Cells* 92 (2008) 136–139.
- [169] K. Doblhofer, *Soft Mater.* 6 (2008) 156–161.
- [170] R.J. Mortimer, *Chem. Soc. Rev.* 1997 (26) (1997) 147–156.
- [171] W. Xu, K. Fu, P.W. Bohn, *ACS Sensors* 2 (2017) 1020–1026.
- [172] M.A. del Valle, L. Ugaldea, F. del Pinoa, F.R. Díaz, J.C. Bernedeb, *J. Braz. Chem. Soc.* 15 (2004) 272–276.
- [173] S. Koyuncu, C. Zafer, E. Sefer, F.B. Koyuncu, S. Demic, I. Kaya, E. Ozdemir, S. Icli, *Synth. Met.* 159 (2009) 2013–2021.
- [174] S. Tarkuc, E. Sahmetlioglu, C. Tanyeli, I.M. Akhmedov, L. Toppare, *Electrochim. Acta* 51 (2006) 5412–5419.
- [175] S. Tarkuc, E. Sahmetlioglu, C. Tanyeli, I.M. Akhmedov, L. Toppare, *Sensors Actuators, B Chem.* 121 (2007) 622–628.
- [176] S. Tirkeş, J. Mersini, Z. Öztas, M.P. Algı, F. Algı, A. Cihaner, *Electrochim. Acta* 90 (2013) 295–301.
- [177] B. Johannsen, M. Scheunemann, H. Spies, P. Brust, J. Wober, R. Syhre, H. J. Pietzsch, *Nucl. Med. Biol.* 23 (1996) 429–438.
- [178] S. Samnick, W. Brandau, J. Sciuk, A. Steinsträßer, O. Schober, *Nucl. Med. Biol.* 22 (1995) 573–583.
- [179] A. Bao, B. Goins, R. Klipper, G. Negrete, W.T. Phillips, *J. Nucl. Med.* 44 (2003) 1992–1999.
- [180] A. Boschi, E. Cazzola, L. Uccelli, M. Pasquali, V. Ferretti, V. Bertolasi, A. Duatti, *Inorg. Chem.* 51 (2012) 3130–3137.
- [181] M. Papadopoulos, I. Pirmettis, C. Tsoukalas, B. Nock, T. Maina, C.P. Raptopoulou, H.J. Pietzsch, M. Friebe, H. Spies, B. Johannsen, E. Chiotellis, *Inorganica Chim. Acta* 295 (1999) 1–8.
- [182] E. Chiotellis, *Inorg. Chem.* 37 (1999) 3212–3218.
- [183] A.P. Borges, B. Possato, A. Hagenbach, A.E.H. Machado, V.M. Deflon, U. Abram, P.I.S. Maia, *Inorganica Chim. Acta* 516 (2021), 120110.
- [184] H.H. Nguyen, P.I.S. Maia, V.M. Deflon, *Inorg. Chem.* 48 (2009) 25–27.
- [185] S. Oya, M.P. Kung, D. Frederick, H.F. Kung, *Nucl. Med. Biol.* 22 (1995) 749–757.
- [186] C. Tsoukalas, M.S. Papadopoulos, T. Maina, I.C. Pirmettis, B.A. Nock, C. Raptopoulou, A. Terzis, E. Chiotellis, *Nucl. Med. Biol.* 26 (1999) 297–304.
- [187] B.A. Nock, T. Maina, D. Yannoukakos, I.C. Pirmettis, M.S. Papadopoulos, E. Chiotellis, *J. Med. Chem.* 42 (1999) 1066–1075.
- [188] A. Zablotskaya, I. Segal, E. Lukevics, S. Belyakov, H. Spies, *Appl. Organomet. Chem.* 21 (2007) 288–293.
- [189] T. Fietz, P. Leibnitz, H. Spies, B. Johannsen, *Polyhedron* 18 (1999) 1793–1797.
- [190] I. Segal, A. Zablotskaya, T. Kniess, I. Shestakova, *Chem. Heterocycl. Compd.* 48 (2012) 296–300.
- [191] J.L. Corbin, K.F. Miller, N. Pariyadath, S. Wherland, A.E. Bruce, E.I. Stiefel, *Inorganica Chim. Acta* 90 (1984) 41–51.
- [192] D. Papagiannopoulou, I. Pirmettis, T. Maina, M. Pelecanou, A. Nikolopoulou, E. Chiotellis, C.P. Raptopoulou, A.T. Vlahos, A. Terzis, M. Papadopoulos, *J. Biol. Inorg. Chem.* 6 (2021) 256–265.
- [193] D. Papagiannopoulou, I. Pirmettis, Ch. Tsoukalas, L. Nikolopoulou, C. Dalla, M. Pelecanou, Z. Papadopoulou-Daifotis, M. Papadopoulos, E. Chiotellis, *Nucl. Med. Biol.* 29 (2002) 825–832.
- [194] P.I.S. Maia, H.H. Nguyen, D. Ponader, A. Hagenbach, S. Bergemann, R. Gust, V. M. Deflon, U. Abram, U. De Sa, *Inorg. Chem.* 51 (2012) 1604–1613.
- [195] P.I.D.S. Maia, Z.A. Carneiro, C.D. Lopes, C.G. Oliveira, J.S. Silva, S. De Albuquerque, A. Hagenbach, R. Gust, V.M. Deflon, U. Abram, *Dalt. Trans.* 46 (2017) 2559–2571.
- [196] A.R. Rettondin, Z.A. Carneiro, A.C.R. Gonçalves, V.F. Ferreira, C.G. Oliveira, A. N. Lima, R.J. Oliveira, S. De Albuquerque, V.M. Deflon, P.I.S. Maia, *Eur. J. Med. Chem.* 120 (2016) 217–226.

- [197] V.A. Kozlov, S.G. Churushova, E.Y. Rybalkina, A.S. Peregodov, G.L. Denisov, D. V. Aleksanyan, *Ineos Open* 2 (2020) 172–177.
- [198] G.G. Mohamed, M.M. Omar, A.M. Hindy, *Turkish J. Chem.* 30 (2006) 361–382.
- [199] H.F. Abd El-Halim, G.G. Mohamed, K. Hofmann, B. Albert, *Comptes Rendus Chim.* 18 (2015) 619–625.



Poonam Kaswan, born in 1987 in Churu (Rajasthan), India, studied at, Indian Institute of Technology Delhi, India and Department of Chemistry, Rajasthan University, Jaipur for her M. Tech. and M.Sc. degree respectively. She is presently pursuing her Ph.D. at the Department of Chemistry, Amity University Haryana under the mentorship of Dr. G. K. Rao.



Preeti Oswal was born in Himachal Pradesh, India in 1995. After receiving B.Sc. and M.Sc. degrees in Chemistry from Shoolini University of Biotechnology and Management Studies, Himachal Pradesh, in year 2017 she became the recipient of a highly prestigious and national-level DST-INSPIRE fellowship (by Department of Science and Technology, Government of India) for pursuing Ph.D. research for five years. She is pursuing her Ph.D. at Department of Chemistry, Doon University, Dehradun under supervision of Dr. Arun Kumar. She is working on developing new chalcogen ligated metal catalysts (homogeneous, heterogeneous and nano-sized) and exploring their applications.



Arun Kumar, a native of Ghaziabad (India), studied at I.I.T. Delhi (2003–2009) for his Ph.D. under the supervision of Prof. A.K. Singh. He has been a recipient of various fellowships (viz. JRF, SRF, RA and SRA) from CSIR India. After joining Doon University, Dehradun in July 2015, he served as the founding Head of the Chemistry Department and Member of the Academic Council and Court of Doon University. He has also been appointed as Coordinator of Innovation Cell of Doon University in February 2021. In addition to completing some research projects (funded by SERB and UGC), he has contributed to publishing 40 articles in international journals of high repute, and 04 book chapters. His h-index is 19 and i-10 index is 25 respectively. Currently, his research group is working on the development of new catalysts and materials for challenging organic transformations.



Chandra Mohan Srivastava received his M.Sc. Chemistry degree from University of Lucknow, M. Tech Plastics Engineering degree from Central Institute of Plastics Engineering & Technology, Lucknow and Ph.D. from Delhi Technological University, Delhi (with Dr. Roli Purwar). He has worked as Lecturer at Central Institute of Plastics Engineering & Technology, Ahmedabad. He is presently working as an Assistant Professor of Chemistry at Amity School of Applied Sciences, Amity University Haryana, India. His research interest includes polymer, biopolymer, nanomaterials for biomedical applications, nanofabrication using electrospinning, and polymer composites. He has published 25 peer reviewed papers, 6 patents and 5 book chapters.



Varun Rawat received his M.Sc. Chemistry degree from the University of Delhi and Ph.D. from CSIR-National Chemical Laboratory, India. He then joined the group of Prof. Arkadi Vigalok as a PBC postdoctoral fellow, where he worked on the synthesis of calixarene-based complexes. He is presently working as a visiting scientist at Tel Aviv University, Israel. His research interest includes the synthesis and application of calixarene-based chemosensors and catalysts. He has published over 20 peer-reviewed papers, 5 patents and 3 book chapters.



Gyandshwar Kumar Rao studied at IIT Delhi for his Ph.D. with Professor Akai Kumar Singh. He worked at the University of Ottawa with Prof. Darrin Richeson as a postdoctoral fellow from 2014-2017. He is currently working as an Assistant Professor at the Department of Chemistry, Amity School of Applied Sciences, Amity University Haryana. His research interest includes the design and synthesis of inorganic, organometallic species and nanomaterials for energy and medicine. He has co-authored of fifty-three research articles published in international journals of high repute, six book chapters and one patent. His H and i-10 index are 20 and 34 respectively.



Dr. Dipti Vaya has awarded Ph. D from MLSU, Rajasthan. She is currently working as an Associated Professor at Department of Chemistry, Amity University Haryana. She has 13 years of teaching and research experience. Her research interests include the development of efficient nanomaterials, polymer nanocomposites, carbon based materials for waste water treatment and water splitting. She was awarded DRDO funded project. She has co-authored various research papers and book chapters of national and international repute.